GR-85-7

ANALOG COMPUTER SIMULATION OF ASWAN HIGH DAM VOLTAGE REGULATORS

September 1985
Engineering and Research Center

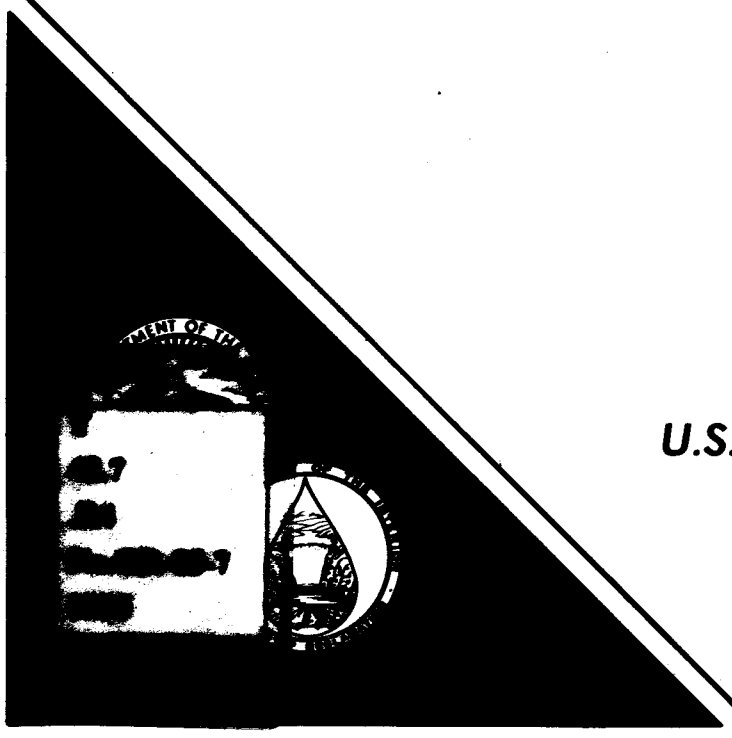

U.S. Department of the Interior
Bureau of Reclamation
Division of Research and
Laboratory Services
Power and Instrumentation Branch

7-2090 (4-81)
Bureau of Reclamation

TECHNICAL REPORT STANDARD TITLE PAGE

1. REPORT NO.	2. GOVERNMENT ACCESSION NO.	3. RECIPIENT'S CATALOG NO.
GR-85-7		

4. TITLE AND SUBTITLE	5. REPORT DATE
Analog Computer Simulation of Aswan High Dam Voltage Regulators	September 1985
	6. PERFORMING ORGANIZATION CODE: D-1550, D-1552
7. AUTHOR(S): J. C. Agee, W. R. Roemish, T. R. Whittemore	8. PERFORMING ORGANIZATION REPORT NO.: GR-85-7
9. PERFORMING ORGANIZATION NAME AND ADDRESS: Bureau of Reclamation, Engineering and Research Center, Denver, CO 80225	10. WORK UNIT NO.
	11. CONTRACT OR GRANT NO.
12. SPONSORING AGENCY NAME AND ADDRESS: Same	13. TYPE OF REPORT AND PERIOD COVERED
	14. SPONSORING AGENCY CODE: DIBR

15. SUPPLEMENTARY NOTES

Microfiche and/or hard copy available at the E&R Center, Denver, Colorado

Ed: RNW (c)

16. ABSTRACT

A report prepared for EEA (Egyptian Electricity Authority) by SWED indicated a need for PSS's (Power System Stabilizers) at Aswan High Dam. This recommendation was based on the results of digital-computer load flow and stability studies, which modeled the voltage regulators as IEEE Type AC4 devices. EEA then asked the USBR to determine whether PSS's would be compatible with their existing voltage regulators furnished by the U.S.S.R. This study describes the modeling techniques and results of an analog computer simulation of the existing voltage regulators. These existing regulators incorporate the PSS function and, therefore, do not need the addition of external PSS's.

17. KEY WORDS AND DOCUMENT ANALYSIS

a. *DESCRIPTORS*-- electric generators/ transmission (electrical)/ power system stability/ electric analogs/ control/ excitation/ *voltage regulators/ stabilization/ *analog models/ machine-control systems

b. *IDENTIFIERS*-- / Aswan High Dam/ Egypt/ voltage regulator/ power system stabilizer

c. *COSATI Field/Group* 09C *COWRR:* 0903 *SRIM:*

18. DISTRIBUTION STATEMENT	19. SECURITY CLASS (THIS REPORT): UNCLASSIFIED	21. NO. OF PAGES: 67
	20. SECURITY CLASS (THIS PAGE): UNCLASSIFIED	22. PRICE

GR-85-7

ANALOG COMPUTER SIMULATION OF ASWAN HIGH DAM VOLTAGE REGULATORS

by

J. C. Agee
W. R. Roemish
T. R. Whittemore

Power and Instrumentation Branch
Division of Research and Laboratory Services
Engineering and Research Center
Denver, Colorado

September 1985

UNITED STATES DEPARTMENT OF THE INTERIOR ★ **BUREAU OF RECLAMATION**

As the Nation's principal conservation agency, the Department of the Interior has responsibility for most of our nationally owned public lands and natural resources. This includes fostering the wisest use of our land and water resources, protecting our fish and wildlife, preserving the environmental and cultural values of our national parks and historical places, and providing for the enjoyment of life through outdoor recreation. The Department assesses our energy and mineral resources and works to assure that their development is in the best interests of all our people. The Department also has a major responsibility for American Indian reservation communities and for people who live in Island Territories under U.S. Administration.

The research covered by this report was funded under the Bureau of Reclamation PRESS (Program Related Engineering and Scientific Studies) allocation No. DR-80, Power System Controls.

PREFACE

This report describes the models used for and the results of a study of the Aswan High Dam Powerplant excitation-control system in Upper Egypt. The study is based on information supplied to the USBR (Bureau of Reclamation) by the EEA (Egyptian Electricity Authority). Detailed information describing the existing parameter settings and operating characteristics of the present excitation-control equipment was not supplied by the EEA. Therefore, this study deals exclusively with a determination of the optimum theoretical performance of the existing equipment with and without additional power system stabilizer equipment. A copy of Activity No. 7 of the SWED POWER Phase II Final Report, dated March 1981, titled "Study on the Improvement of the Reliability of the 500-kV Transmission System from the High Dam to the Cairo Region and the Possibilities to Increase the Firm Transmission Capacity," [1]* was used to validate the results obtained from the Controls Section analog computer model.

This report was prepared by the Controls Section of the Power and Instrumentation Branch of the Division of Research and Laboratory Services. It is one of a series of reports documenting hydroelectric synchronous machine-control system modeling studies. The Controls Section is involved in the development of analog and digital computer models, field testing and alignment of synchronous machine-control systems, and applied research into improved control techniques. Members of the Controls Section are active in WSCC (Western Systems Coordinating Council) and IEEE (Institute of Electrical and Electronic Engineers) subcommittees developing standards for modeling and testing of synchronous machine-control systems.

* Numbers in brackets refer to the bibliography.

GLOSSARY OF SYMBOLS AND ACRONYMS

Symbols

δ = torque angle

$E(MWS)$ = total kinetic energy of inertia

E_{Bd} = direct-axis component of infinite-bus voltage phasor

E_{Bq} = quadrature-axis component of infinite-bus voltage phasor

$\overrightarrow{E}_{Bus}$ = infinite-bus voltage phasor

E_{md} = direct-axis component of midpoint-bus voltage phasor

$\overrightarrow{E}_{mid}$ = midpoint-bus voltage phasor

E_{mq} = quadrative-axis component of midpoint-bus voltage phasor

H = inertia constant

$\overrightarrow{I}_B$ = infinite-bus current phasor

I_d, I_{td} = direct-axis component of machine-current phasor

$\overrightarrow{I}_L$ = midpoint-load current phasor

I_{Ld} = direct-axis component of midpoint-load current phasor

I_{Lq} = quadrature-axis component of midpoint-load current phasor

I_q, I_{tq} = quadrature-axis component of machine-current phasor

$\overrightarrow{I_t}$, $\overrightarrow{I}$ = machine-current phasor

$K_{\Delta v}$ = voltage regulator gain of terminal voltage deviation

$K_{v'}$ = voltage regulator gain of derivative of terminal voltage

K_{It} = voltage regulator gain of line current

$K_{I't}$ = voltage regulator gain of derivative of line current

$K_{I''t}$ = voltage regulator gain of second derivative of line current

$K_{I'R}$ = voltage regulator gain of derivative of rotor current

K_{FDBKt} = voltage regulator gain of derivative of field voltage

K_{FDBKd} = voltage regulator gain of field current

P_e = electrical power

P_m = mechanical power

$S_{G1.0}$ = generator saturation at rated terminal voltage

$S_{G1.2}$ = generator saturation at 1.2 times rated terminal voltage

T''_{DO} = direct-axis subtransient open-circuit time constant

T''_{QO} = quadrature-axis subtransient open-circuit time constant

T'_{DO} = direct-axis transient open-circuit time constant

T_m = generator mechanical time constant

$\overrightarrow{V}_t$ = terminal-voltage phasor

V_{td} = direct-axis component of terminal-voltage phasor

V_{tq} = quadrature-axis component of terminal-voltage phasor

X = system equivalent reactance

X''_D = direct-axis subtransient reactance

X''_Q = quadrature-axis subtransient reactance

X'_D = direct-axis transient reactance

X_B = equivalent reactance from midpoint bus to infinite bus

X_D = direct-axis synchronous reactance

X_L = armature-leakage reactance

X_{Line} = equivalent reactance from machine to midpoint bus

X_Q = quadrature-axis synchronous reactance

GLOSSARY OF SYMBOLS AND ACRONYMS – Continued

Acronyms

EEA = Egyptian Electricity Authority
IEEE = Institute of Electrical and Electronic Engineers
PSS = Power System Stabilizer
SWED = Swedish Power Service
WSCC = Western Systems Coordinating Council

CONTENTS

TABLES

FIGURES

CONTENTS – Continued

INTRODUCTION

As a part of Activity No. 7 of the SWED Phase II Final Report [1], dated March 1981, performed for EEA, a recommendation was made to install PSS's (power system stabilizers) at Aswan High Dam. This recommendation was based on the results of digital-computer load flow and stability studies, which modeled the voltage regulators as IEEE Type AC4 devices. EEA then asked the USBR to determine whether PSS's were compatible with their existing voltage regulators furnished by the U.S.S.R. This study was undertaken to determine the effect of the existing voltage regulators on power system stability and to explore the addition of PSS's.

CONCLUSIONS

The existing Russian regulators are not simply voltage-regulating devices. They incorporate feedback from the terminal voltage, the derivative of terminal voltage, the 500-kV line current, the first and second derivatives of line current, and the derivative of rotor (field) current. Therefore, if properly aligned, these regulators can contribute to the dynamic stability of the power system and to its steady-state and transient stability. A typical IEEE Type AC4 voltage regulator increases only the transient and steady-state stability of the power system and decreases the dynamic (power-oscillation) stability limit. By adding a PSS to the type AC4 regulator, dynamic stability can be increased while retaining the increased transient and steady-state limits. By using additional feedback quantities, the existing High Dam regulators incorporate these dynamic-stability considerations.

Unanswered questions center on the alignment of the existing High Dam regulators and the typical system conditions. If the current-feedback quantities are not properly adjusted, the dynamic stability of the system could be worse than it would be without these quantities. The alignment also depends on the oscillation modes of the system. A strong mode between Aswan High Dam and Aswan Power Stations could hinder efforts to stabilize the 500-kV system; however, the use of 500-kV line current, rather than generator current, input to the regulator should eliminate this problem.

A record of actual line flows on the High Dam-Nag Hammadi, the Nag Hammadi-Samalut, and the Samalut-Cairo sections that show the damping or development of oscillations would help validate the model results. The SWED report seems to give conservative line limits based on the study of the actual voltage-regulating equipment. PSS's do not seem to be needed with the existing regulators; however, if these regulators are replaced with conventional equipment, there will be a definite need for PSS's.

BACKGROUND

The Egyptian power system of concern consists of thermal generation in the Cairo area in Lower Egypt and hydroelectric generation at the Aswan High Dam, Aswan, and Aswan II Powerplants in Upper Egypt. The system data were taken from the forecast for the 1985 system conditions in the SWED report.

The generation capacity in Upper Egypt is approximately 3070 MV·A, and the capacity in the Cairo area is approximately 4770 MV·A. The major load is in the Cairo area. The Upper Egypt generation is connected to the load in the Cairo area by two 500-kV transmission lines. There is limited generation at Assiut (110 MV·A), a midpoint on the 500-kV transmission line.

The load in Upper Egypt is predominately at Nag Hammadi and is less than 25 percent of the capacity in Upper Egypt. Nearly 50 percent of the capacity in Upper Egypt goes unused unless it is transmitted to the Cairo area. The present system can transmit less than 25 percent of the capacity of Upper Egypt to Cairo. The objective is to increase this percentage.

The problem is similar to a classical stability problem, in which two large masses are connected by a weak spring. The inertia of the Cairo area system is nearly the same as the inertia of the system in Upper Egypt. There is more generation in the Cairo area, but the inertia of the individual steam generators there is less than that of the individual hydroelectric generators in Upper Egypt. The two 500-kV lines provide the only tie between these two large inertias. The limiting case for stability analysis is the system condition in which one of two parallel line sections is out of service. In this limiting case the tie is weak.

The SWED study addresses several methods for improving the stability of the system and increasing the transmission to Cairo. One of the proposed solutions involves the addition of PSS's. This study attempts to validate the recommendation that PSS's be used.

GENERATOR MODEL

Figure 1 shows the 2-axis machine model used in this study. This model is described in detail in [2]. Table 1 shows the parameters used in this model. X''_q was unavailable in the SWED report; therefore, a value equal to X''_d was used.

The model chosen uses inputs of direct- and quadrature-axis machine currents and applied field voltage. The model outputs values of direct- and quadrature-axis machine voltage. The tieline model used is compatible with this approach.

Figure 2 shows the open-circuit saturation curve for the High Dam units based on the parameters $S_{G1.0}$ and $S_{G1.2}$ given in the Swedish study. Table 2 lists the function generator values used in the model.

TIELINE AND INFINITE-BUS MODEL

Figure 3 shows the tieline and infinite-bus representation initially used in this study. The swing equation is represented by amplifiers A35, A34, and A36 and potentiometers P36, P37, and P17. This group of elements solves the torque angle equation:

$\delta = \int 314 \int \frac{P_m - P_e}{T_m}$, when the damping constant, represented by P17, is set to zero.

The damping constant, P17, is incorporated in the model to determine the relative stability. Negative damping can be inserted until a normally stable system begins to oscillate. This allows measurement of the damping in a stable system.

Amplifiers A3, A13, A41, and A45 create electrical power from the terminal direct- and quadrature-axis voltages and currents. Mechanical power from the turbine is assumed to be constant for the range of oscillation frequencies that voltage regulators cause. This is represented by P16.

The output of the swing equation is the total angle between the machine quadrature axis and the infinite-bus voltage phasor. This angle allows the infinite-bus voltage to be decomposed into its direct- and quadrature-axis components. At this point the tieline equation shown on figure 4 can be solved. This equation can be stated in direct- and quadrature-axis form as follows:

$$\vec{V_t} = \vec{jI}X + \vec{E}_{Bus}$$

$$(\vec{V_{td}} + j\vec{V_{tq}}) = jX(\vec{I_d} + \vec{jI_q}) + (\vec{E}_{Bd} + j\vec{E}_{Bq})$$

$$\vec{V_{td}} = -X\vec{I_q} + \vec{E}_{Bd}$$

$$\vec{V_{tq}} = + X\vec{I_d} + \vec{E}_{Bq}$$

These equations are solved using amplifiers A51, A55, A103, and A113 and potentiometers P61, P74, and P75. Switches S51 and S55 provide a means to take the generator off line for testing.

During the testing it was determined that a midpoint load was needed so that the identities of the High Dam-Cairo power flow and impedance were not lost in the total system representation. The model section on figure 5 was installed for this purpose. This model applies a constant current load at a point between the machine and the infinite bus. It was necessary to back-calculate the values of midpoint voltage and infinite-bus current to avoid numerical instability when using high tieline-impedance values. The equations for the midpoint load system are as follows:

$$\vec{V}_t = \vec{E}_{mid} + j\vec{I}_t X_{Line} \quad \rightarrow \quad \vec{V}_t - j\vec{I}_t X_{Line} = \vec{E}_{mid}$$

$$\vec{E}_{mid} = \vec{E}_{Bus} + j\vec{I}_B X_B \quad \rightarrow \quad \frac{\vec{E}_{mid} - \vec{E}_{Bus}}{jX_B} = \vec{I}_B$$

$$\vec{I}_t = \vec{I}_B + \vec{I}_L$$

$$\vec{I}_t = \frac{\vec{E}_{mid}}{jX_B} - \frac{E_{Bus}}{jX_B} + \vec{I}_L$$

$$\vec{I}_t = \frac{\vec{V}_t}{jX_B} - \frac{j\vec{I}_t X_{Line}}{jX_B} - \frac{\vec{E}_{Bus}}{jX_B} + \vec{I}_L$$

$$\vec{I}_t + \vec{I}_t \frac{X_{Line}}{X_B} = \frac{\vec{V}_t}{jX_B} - \frac{\vec{E}_{Bus}}{jX_B} + \vec{I}_L$$

$$\vec{I}_t = \frac{\vec{V}_t}{jX_B\,(1 + X_{Line}/X_B)} - \frac{\vec{E}_{Bus}}{jX_B\,(1 + X_{Line}/X_B)} + \frac{\vec{I}_L}{(1 + X_{Line}/X_B)}$$

$$\vec{I}_t = \frac{\vec{V}_t}{j(X_B + X_{Line})} - \frac{\vec{E}_{Bus}}{j(X_B + X_{Line})} + \frac{\vec{I}_L X_B}{(X_B + X_{Line})}$$

$$\vec{I}_{td} + j\vec{I}_{tq} = \frac{\vec{V}_{td}}{j\,(X_B + X_{Line})} + \frac{j\vec{V}_{tq}}{j\,(B_B + X_{Line})} - \frac{\vec{E}_{Bd}}{j(X_B + X_{Line})} - \frac{j\vec{E}_{Bq}}{j(X_B + X_{Line})} + \frac{\vec{I}_{Ld} X_B}{X_B + X_{Line}} + \frac{j\vec{I}_{Lq} X_B}{X_B + X_{Line}}$$

$$\vec{I}_{td} = \frac{\vec{V}_{tq}}{X_B + X_{Line}} - \frac{E_{Bq}}{X_B + X_{Line}} + \frac{\vec{I}_{Ld} X_B}{X_B + X_{Line}}$$

$$\vec{I}_{tq} = \frac{-V_{td}}{X_B + X_{Line}} + \frac{\vec{E}_{Bd}}{X_B + X_{Line}} + \frac{\vec{I}_{Lq} X_B}{X_B + X_{Line}}$$

$$\vec{E}_{md} = \vec{V}_{td} + \vec{I}_{tq}X_{Line}$$

$$\vec{E}_{mq} = \vec{V}_{tq} - I_{td}X_{Line}$$

Figure 6 shows the single-line diagram of this system.

CALCULATION OF INERTIA CONSTANT

The equivalent inertia constant, *H*, for the High Dam-Cairo system when converting the equivalent two-finite-machine system to an equivalent finite-infinite machine system calculated as:

	Rating MV·A	*H*	Study Power	*H* on 2060 MV·A_{Base}
High Dam	2060	7.41	1700	
Aswan II A	150	3.3	136	
Aswan II B	150	3.3	136	
Aswan I	297	4.4	222	
U. Egypt Equiv.	2657	6.61	2194	8.52
L. Egypt Equiv.	4164	2.85	3305	
Assiut	112.5	4.0	90	
Ayat	600	4.0	316	
L. & M. Egypt Equiv.	4877	3.02	3711	7.15
Total System (U., L. & M. Egypt)	7534	4.29	5905	

$$H = \frac{E\ (MWS)}{S_{Base}}$$

$$H_{eq} = \frac{H_u H_L}{H_u + H_L} = 3.89 \text{ on } 2060 \text{ MV} \cdot A_{Base}$$

Note that the kinetic energy of Upper Egypt is 22,638 MJ; whereas, the kinetic energy of Lower Egypt is only 14,729 MJ. Thus, Aswan High Dam more closely approximates an infinite mass than does Cairo.

EGYPTIAN POWER SYSTEM MODEL

The basis for the power system model used was found in appendix 1 of the Swedish study. Figure 7 shows these data on a diagram of the 500-kV system. Appendix A of this report shows a network reduction for this system. The resulting equivalent finite machine-to-infinite bus system has a reactance between machine model Thevenin voltages of 0.673 per unit (on a 2060 $MV \cdot A_{Base}$) with both High Dam-Nag Hammadi lines in service or a reactance of 0.784 per unit with one line out of service. Unfortunately, this model is inaccurate because the total power generated in Upper Egypt is not transmitted through the equivalent reactance of the model. Therefore, an intermediate load was added to the transmission system (at Nag Hammadi) to more accurately model the Egyptian 500-kV system. Figure 8 shows the system chosen to model the 500-kV system more accurately. Results obtained with this model corroborate the Swedish report much better than those obtained with the simple machine infinite-bus system having no intermediate load.

IEEE TYPE AC4 REGULATOR MODEL AND RESULTS

Figure 9 shows the block diagram of the regulator model used in the Swedish study. This diagram fits the form of the IEEE Type AC4 model [3]. Figure 10 shows the analog computer representation used in this study.

First, off-line data were gathered using the IEEE Type AC4 regulator. Figure 11 shows the off-line time-domain performance of this regulator with varying amounts of gain. Figure 12 shows the closed-loop frequency response of this regulator with the gain set to 31 (the value used in the SWED study).

Figure 13 shows the on-line time-domain performance of the regulator when the generator is running at no load. Note that as the line impedance increases, the gain of the overall excitation system increases also.

For the finite-machine tieline, infinite-bus system on figure 4, the regulator gave the results shown on figure 14. Table 3 summarizes the synchronizing-power coefficient and damping-power coefficients observed in these and other tests.

It was noticed that the oscillation frequencies obtained in this study did not match the frequencies found in the SWED report. It seems that combining all of the 500-kV system into a single equivalent voltage and impedance is not adequate for maintaining the correct swing frequency. Therefore, a frequency-domain technique was used to discover the effect of voltage-regulator action on damping power.

Figure 15 shows Bode plots of the machine transfer function, P_e/δ. It should be noted that any time the machine has a lagging phase angle, the overall machine tieline-infinite bus system is unstable. On figure 15 (sheet 1) this region can be observed as swing frequencies below 0.075 Hz (with a regulator gain of 31). Figure 15 (sheet 2) indicates that as machine power increases, the frequency range of unstable operation increases. At 1.0 per unit (on a 2060 $MV \cdot A_{Base}$) power, the machine is unstable for swing frequencies below 0.95 Hz. This result can also be seen in table 3.

Unfortunately, this frequency-response technique provides no insight into power transfers or system configuration. However, it is a powerful tool for pointing out frequencies at which sufficient damping is unavailable. The oscillation modes within regions that are actually present on the system depend on the particular system configurations used.

To investigate actual line flows, the system on figure 6 was connected. Figure 16 shows a phasor diagram of the system with both High Dam-Nag Hammadi lines in service, and figure 17 shows a phasor diagram with one line out of service. With both lines in service, the transfer from High Dam-Nag Hammadi was limited to 1700 MW, and the transfer from Nag Hammadi-Cairo was 1025 MW. The oscillation frequency observed was 0.72 Hz under these conditions. Figure 18 shows this condition.

With one High Dam-Nag Hammadi line out of service, the power transfer from High Dam-Nag Hammadi was limited to 1350 MW, and the Nag Hammadi-Cairo transfer was 660 MW. The oscillation frequency for this case was 0.63 Hz. Figure 19 shows this case.

Unfortunately, direct comparison of the findings of this study with those of the SWED study cannot be made because of the inability to model many machines on the analog computer and the unavailability of most of the SWED study load-flow data. (Only two cases are included in the appendices of the SWED Report). However, the findings in this section are reasonably close to the SWED study summary of 1700 MW for both lines in service and 1550 MW with one line out of service.

POWER SYSTEM STABILIZER

A PSS of the speed type was connected to the Type AC4 regulator model by using the analog diagram of figure 20. The resulting power-transfer increase is shown in table 4 for various stabilizer gain settings. In real applications this gain will be limited by local plant swing modes. This limitation is not now known. From examining the SWED study, it appears that a gain of 1.5 per unit was used. If that was the case, a transfer increase of about 150 MW would be obtained as stated in the SWED study.

EXISTING REGULATOR MODEL AND RESULTS

A block diagram of the existing Aswan High Dam regulators is shown on figure 21 [4]. The inputs from derivatives of line current, terminal voltage, and field current make this an extremely difficult regulator to understand and align. The analog model used is shown on figure 22. Terminal voltage and current were obtained by using vector modules remote from the analog computer. Direct- and quadrature-axis voltages and currents were input to the vector modules, and the terminal quantities were output.

An off-line alignment of this regulator was done by using the derivative of voltage. This adjustment provided a sort of transient gain reduction. Figure 23 shows the off-line time-domain response of this regulator for various values of K_V. Figure 24 shows the on-line no-load time-domain responses of this regulator with various line impedances.

The on-line alignment of the current feedback elements was made by loading the unit into the machine, infinite-bus, midpoint load system and adjusting the parameters until a damping improvement was seen. Table 5 shows the power transfer limits for various regulator parameters. Actual parameters in use on the regulators would be helpful to this part of the study.

The frequency-response technique presented earlier was also used with the existing regulator. Figure 25 shows that for low values of line impedance (approximately 25%) to the infinite bus, the High Dam regulators would be unstable at frequencies above 1.0 Hz. There appears to be a significant increase in damping at frequencies below 1 Hz for all values of impedance. This is an interesting phenomenon, which should be investigated further.

BIBLIOGRAPHY

[1] "Study on the Improvement of the Reliability of the 500-kV Transmission System from the High Dam to the Cairo Region and the Possibilities to Increase the Firm Transmission Capacity," SWED POWER Phase II Final Report, March 1981.

[2] PTI Course Notes, "Power System Dynamics: Volume 1," Power Technologies, Inc., Schenectady, New York, 1978.

[3] "Excitation System Models for Power System Stability Studies," IEEE Committee Report, IEEE Transactions on Power Apparatus and Systems, Vol. PAS-100, No. 2, February 1981.

[4] "Main Generator Automatic Voltage Regulator Type АРГГ-ТС," V. I. Lenin All-Union Electrotechnical Institute, Moscow, U.S.S.R.

Table 1. – Aswan High Dam synchronous machine parameters.

	SWED	Brown Boveri	Model Data Used
X_D	1.1025	1.0	1.1025
X_Q	0.6615	0.66	0.6615
X'_D	0.3638	0.33	0.3638
X''_D	0.2392	0.22	0.2392
X''_Q	N/A	0.33	0.24
X_L	0.1690	N/A	0.169
T'_{DO}	8.5	2.8	8.5
T''_{DO}	0.06	0.15	0.06
T''_{QO}	0.1	N/A	0.1
$MV \cdot A_{Base}$	171.7 each	206 each	171.7 each
$S_{G1.0}$	0.0857	N/A	0.0857
$S_{G1.2}$	0.2432	N/A	0.2432

Table 2. – Saturation curve function generator values.

GENERATOR SATURATION - ASWAN HIGH DAM

SG=B*(Et-A)*(Et-A)/Et
A= .763415467333 B= 1.53111610898
SG1.0= .0857 SG1.2= .2432

Et (PU)	SAT FUNC Sg (PU)	Sg*Efd (PU)	(1+Sg)*Et (PU
0	0	0	0
.05	0	0	.05
.1	0	0	.1
.15	0	0	.15
.2	0	0	.2
.25	0	0	.25
.3	0	0	.3
.35	0	0	.35
.4	0	0	.4
.45	0	0	.45
.5	0	0	.5
.55	0	0	.55
.6	0	0	.6
.65	0	0	.65
.7	0	0	.7
.75	0	0	.75
.8	2.56161089769E-3	2.04928871815E-3	.80204928872
.85	1.35042302602E-2	1.14785957212E-2	.86147859572
.9	3.17372036323E-2	.028563483269	.928563483268
.95	5.61094224863E-2	.053303951362	1.00330395137
1	8.56999999997E-2	8.56999999998E-2	1.0857
1.05	.119763456364	.125751629182	1.17575162918
1.1	.157689853555	.173458838911	1.27345883892
1.15	.198975329723	.228821629182	1.37882162918
1.2	.2432	.29184	1.49184
1.25	.29001116109	.362513951363	1.61251395136
1.3	.339110371745	.440843483268	1.74084348328
1.35	.390243404238	.526828595723	1.87682859573
1.4	.443192349084	.620469288718	2.02046928871
1.45	.497769353281	.721765562258	2.17176556226
1.5	.553811610897	.830717416345	2.33071741635
1.55	.611177323212	.947324850978	2.49732485098
1.6	.669742416344	1.07158786615	2.67158786615
1.65	.729397855685	1.20350646188	2.8535064619
1.7	.7900474342	1.34308063814	3.04308063815
1.75	.851605939977	1.49031039496	3.24031039498
1.8	.913997629067	1.64519573232	3.44519573233
1.85	.977154946065	1.80773665022	3.65773665023
1.9	1.04101744667	1.97793314867	3.87793314868
1.95	1.10553088598	2.15578522766	4.10578522765
2	1.1706464436	2.3412928872	4.3412928872

Table 3. – Summary of synchronizing and damping power coefficients.

$S_p = P_{max} \cos \delta$ $\quad P_{max} \approx \frac{E_{Bus}\, E_{fd}}{X_q + X_{Line}}$ $\quad \omega_n = \sqrt{\frac{\omega_s\, S_p}{2H}}$ $\quad \omega_s$ (50 Hz) = 314.16

H_{eq} (Aswan High Dam with system effects) = 3.31 $\quad K_S = \frac{\pi H}{15\ T_{osc}}$ $\quad K_D = \frac{4H}{t_d}$

								Data Records		Actual	
X_{Line}	$X_{Line} + X_q$	E_{fd}	$\approx P_{max}$	δ @ 1.0 pu load	S_p	ω_n	f_n	K_s	K_D	f_n	K_D
0.25	0.91	1.55	1.70	46.1°	1.18	7.5	1.19	0.94	6.3	1.36	6.62
.30	.96	1.58	1.65	48.7°	1.09	7.2	1.14	.90	5.9	1.30	5.50
.35	1.01	1.61	1.59	51.3°	0.996	6.9	1.09	.86	4.4	1.24	4.42
.40	1.06	1.64	1.55	53.9°	.913	6.6	1.05	.83	3.7	1.20	3.74
.45	1.11	1.67	1.50	56.7°	.824	6.3	0.995	.79	2.9	1.14	2.87
.50	1.16	1.70	1.47	59.5°	.745	5.9	.95	.76	2.2	1.095	2.20
.60	1.26	1.77	1.41	65.6°	.582	5.3	.84	.68	1.2	0.98	1.04
.70	1.36	1.86	1.36	72.2°	.418	4.5	.71	.60	0.08	.86	0.09

H	$X_{Line}+X_q$	E_{fd}	$\approx P_{max}$	δ $\quad$ P_e	S_p	ω_n	f_n	K_s	K_D	f_n	K_D
3.31	1.36	1.86	1.36	72.2° @ 1.0	0.418	4.5	0.71	0.60	0.08	0.86	0.09
4.0	1.36	1.85	1.36	71.9° @ 0.996	.42	4.07	.65	0.65	0	.78	0
5.0	1.36	1.82	1.34	70.7° @ .98	.44	3.73	.59	0.75	0	.71	0
6.0	1.36	1.80	1.32	69.6° @ .96	.46	3.48	.55	0.83	0	.66	0
7.0	1.36	1.79	1.32	68.9° @ .95	.47	3.26	.52	0.89	0	.61	0
8.0	1.36	1.78	1.31	68.6° @ 0.95	.48	3.06	.49	0.96	0	.57	0

Table 4. – Results of study with IEEE type AC4 regulator.

(a) One line out of service

PSS Gain	HD-NH	NH-Cairo	NH Load
10.0	1747 MW	1178 MW	569 MW
5.0	1683 MW	1079 MW	604 MW
2.0	1524 MW	873 MW	651 MW
1.0	1442 MW	775 MW	667 MW
0.0	1350 MW	660 MW	690 MW

(b) Both lines in service

PSS Gain	HD-NH	NH-Cairo	NH Load
10.0	>2200 MW	>1600 MW	600 MW
5.0	2125 MW	1503 MW	622 MW
2.0	1920 MW	1261 MW	661 MW
1.0	1788 MW	1108 MW	680 MW
0.0	1700 MW	1025 MW	675 MW

Table 5. – Results of study with existing regulator.

(a) One line out of service

Conditions	HD-NH	NH-Cairo	NH Load
No current FB $K_{\Delta V} = 25$ $K_{V'} = 10$	1154 MW	453 MW	700 MW
$K_{It} = 0.25$ pu $K_{Pt} = 5.0$ pu $K_{Pt} = 0.0$ pu	1298 MW	618 MW	680 MW
$K_{It} = 0.25$ pu $K_{Pt} = 5.0$ pu $K_{Pt} = -2.5$ pu	1732 MW	1151 MW	581 MW
$K_{It} = 0.25$ pu $K_{Pt} = 5.0$ pu $K_{Pt} = -1.0$ pu	1655 MW	1046 MW	609 MW

(b) Both lines in service

Conditions	HD-NH	NH-Cairo	NH Load
No current FB $K_{\Delta V} = 25$ $K_{V'} = 10$	1400 MW	713 MW	690 MW
$K_{It} = 0.25$ pu $K_{Pt} = 5.0$ pu $K_{Pt} = 0.0$ pu	1755 MW	1079 MW	676 MW
$K_{It} = 0.25$ pu $K_{Pt} = 5.0$ pu $K_{Pt} = -2.5$ pu	2190 MW	1580 MW	610 MW
$K_{It} = 0.25$ pu $K_{Pt} = 5.0$ pu $K_{Pt} = -1.0$ pu	2108 MW	1482 MW	626 MW

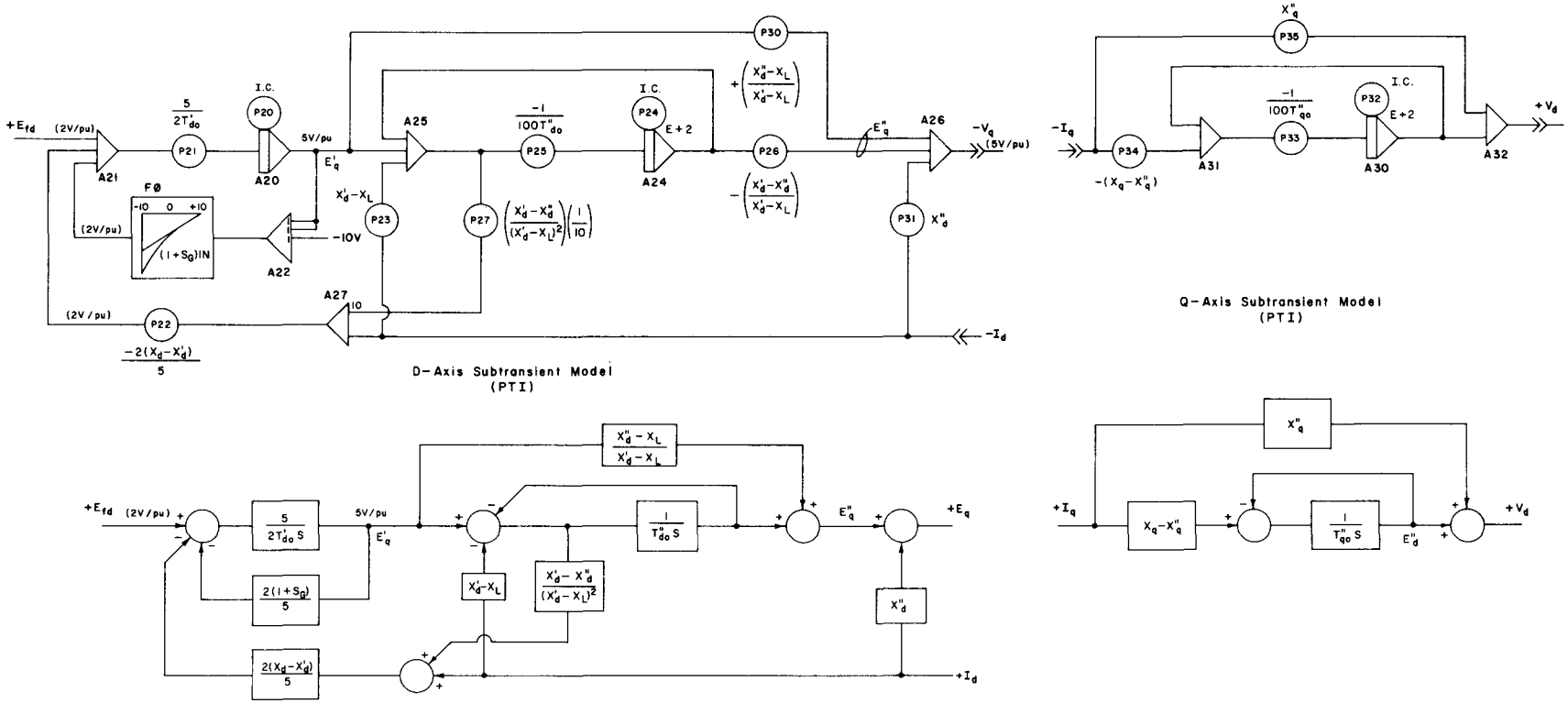

Figure 1. – Two-axis synchronous machine model.

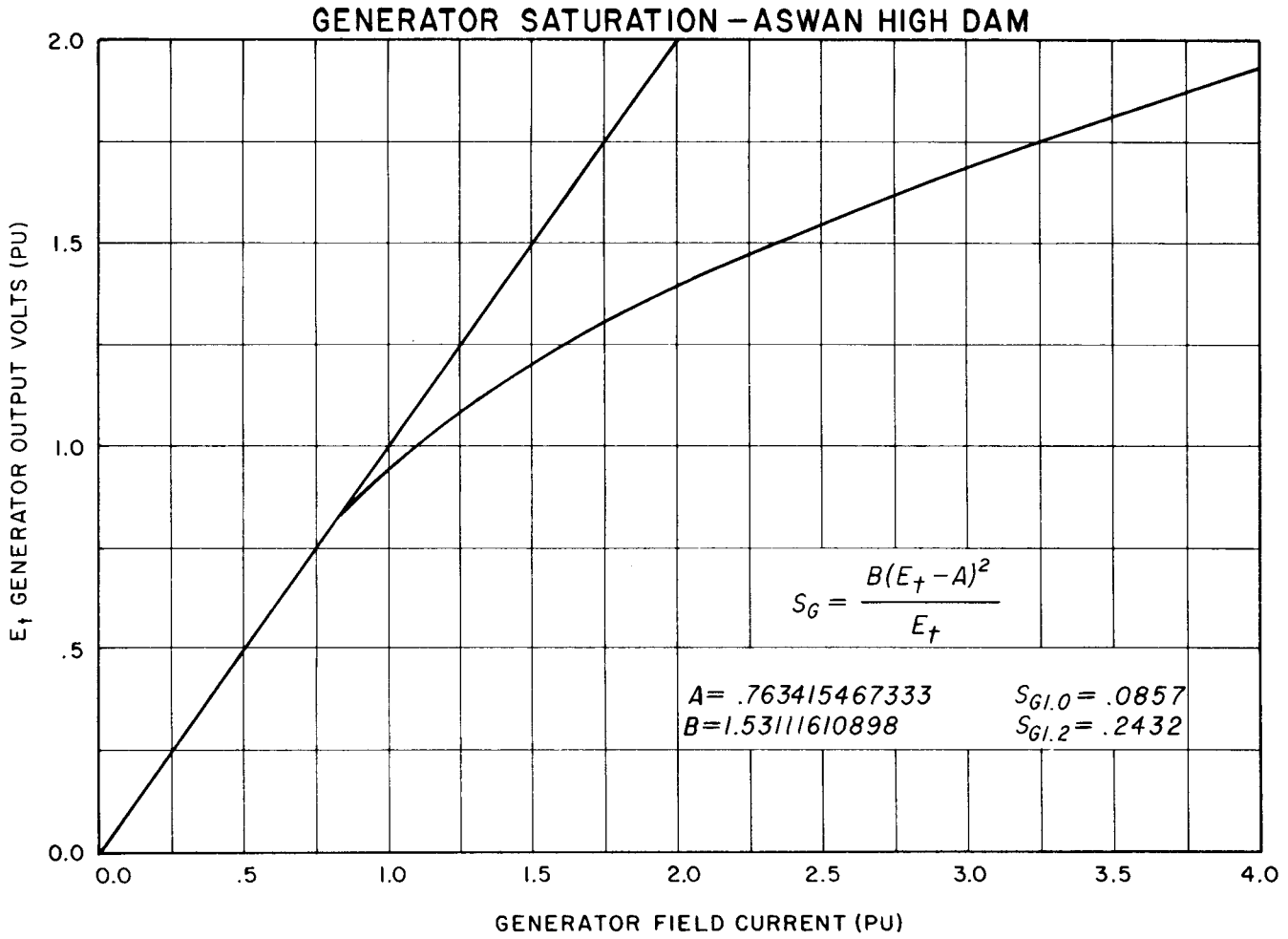

Figure 2. – Open-circuit saturation curve.

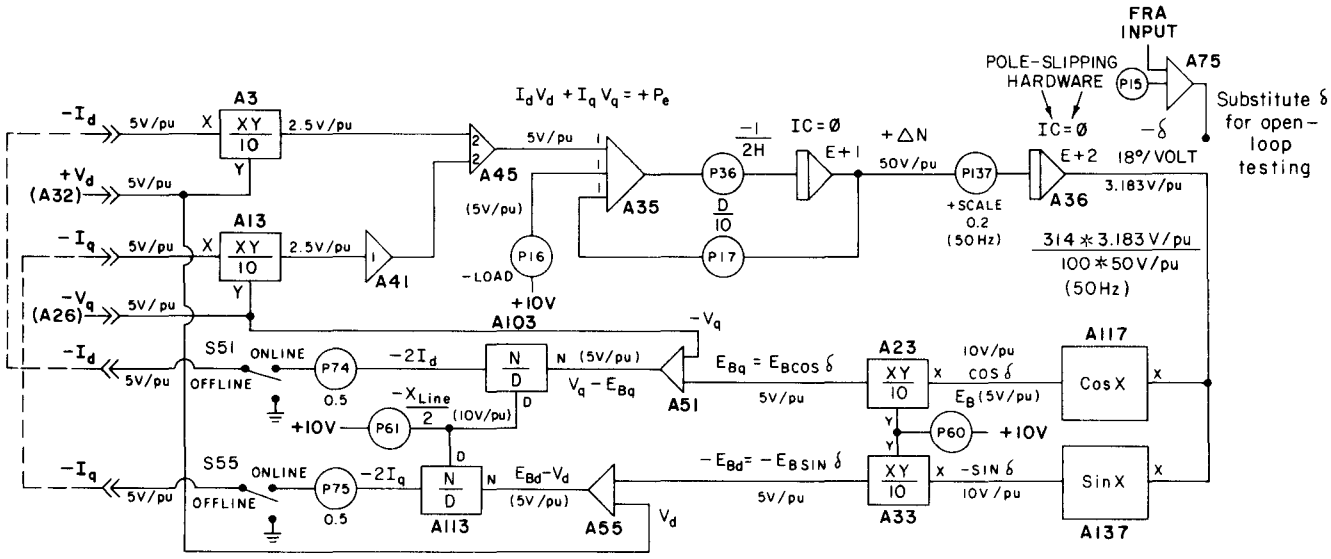

Analog Trunks and Variables

$+V_d$	401	from	A 32
$-V_q$	402	from	A 26
$-I_d$	403	from	A103
$-I_q$	404	from	A113
V_t	1	from	Vector Module
I_t	3	from	Vector Module
$+P_e$	from	A45	(5 V/pu)
$+\Delta N$		A34	(50 V/pu)
$-\delta$		A36	18°/V
E_B		P60	5 V/pu
$-X_L$		P61	10 V/pu

Integrators

I 0	I'_t	ckt.	E + 0
I 4	E_{fd}	2V/pu	E + 1
I10	dV/dt	ckt.	E + 0
I14	rate FB	ckt.	E + 0
I16	I''_t	ckt.	E + 0
I20	E'_q	5 V/pu	E + 0
I24	E''_q	5 V/pu	E + 2
I30	E''_d	5 V/pu	E + 2
I34	$+\Delta N$	50 V/pu	E + 1
I36	$-\delta$	18°/V	E + 2

Coefficients

C 0	K_I	(AVR)
C 1	K'_I	(AVR)

Coefficients - Continued

C 2	K''_I	(AVR)
C 3	$-K_{E_{fd}}$	(AVR)
C 4	$-K_f$	(AVR)
C 5	$+1/100/T_f$	(AVR)
C 6	$-K'_v$	(AVR)
C 7	Manual Excitation	(AVR)
C10	-Ref.	(AVR)
C11	-I.C. of E_{fd}	(AVR)
C12	+I.C. of E_{fd}	(AVR)
C13	+I.C. of V_t	(AVR)
C14	$-1/10\ T_A$	(AVR)
C15	Substitute δ	(Open loop testing)
C16	$-P_{load}$	(Swing Eq.)
C17	D/100	(Swing Eq.)
C20	-I.C. of E'_q	(D-Axis) $[-V_t]$
C21	$\frac{5}{2T'_{do}}$	(D-Axis)
C22	$\frac{-2\,(X_d - X'_d)}{5}$	
C23	$X'_d - X_L$	
C24	+I.C. of E''_q	(D-Axis) $[V_t]$
C25	$\frac{-1}{100\,T''_{do}}$	
C26	$-\left(\frac{X'_d - X''_d}{X'_d - X'_L}\right)$	
C27	$-\left(\frac{X'_d - X''_d}{(X'_d - X'_L)^2}\right)$	
C30	$\frac{X''_d - X_L}{X'_d - X_L}$	
C31	X''_d	
C32	I.C. of E''_d $[V_d]$	
C33	$\frac{-1}{100\,T''_{qo}}$	
C34	$-(X_q - X''_q)$	
C35	X''_q	
C36	$\frac{-1}{T_m}$	Swing Eq.
C37	+ Scale (0.2)	Swing Eq. Int.
C40	-9.85 V	Int. Reset Ckt.
C41	+9.85 V	Int. Reset Ckt.
C44	+9.9 V	Int. Reset Ckt.
C45	-	
C50	Step Input	
C51	-	
C54	-	
C55	-	
C60	$+E_B$	(5 V/pu)
C61	$-X_L$	(10 V/pu)
C64	-	
C65	V_t	correction - 0.003pu
C70	-	
C71	-	
C74	Pu correction	
C75	Pu correction	

Figure 3. – Tieline and infinite-bus model.

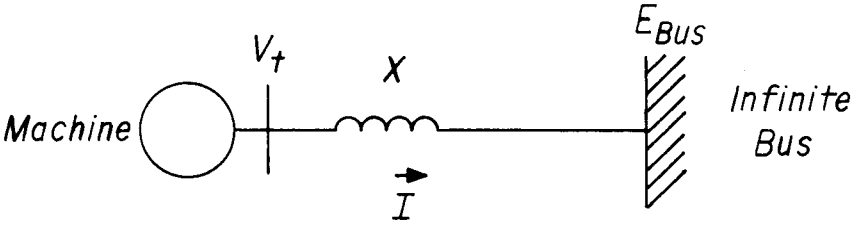

$$\vec{V_t} = j\vec{I}X + \vec{E}_{Bus}$$

Figure 4. – Tieline single-line diagram and equation.

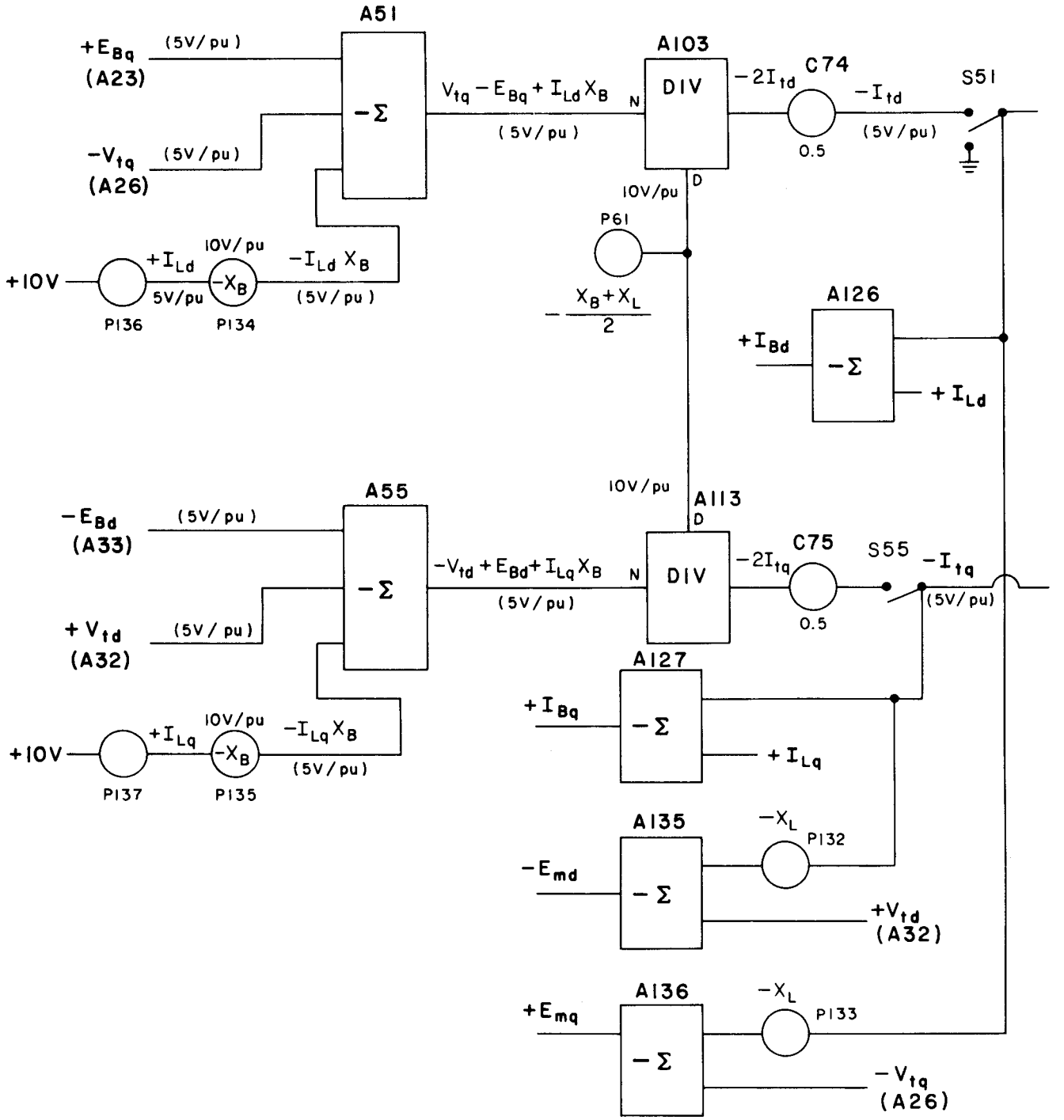

Figure 5. – Analog computer diagram for midpoint load.

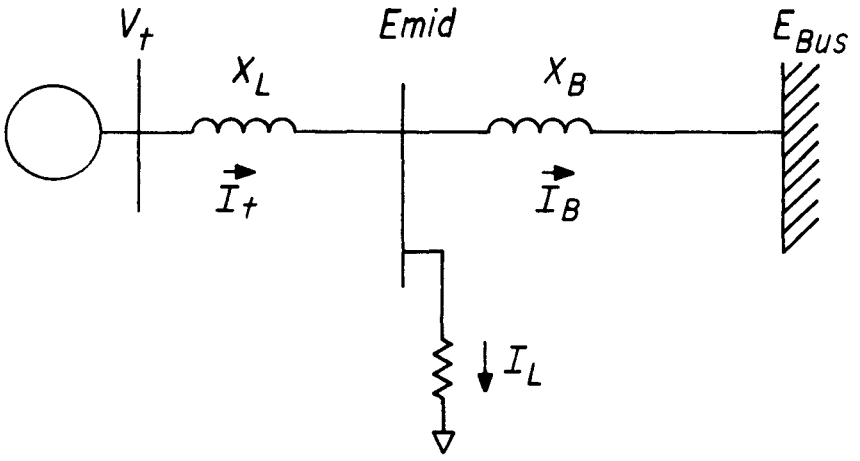

Figure 6. – Single-line diagram of the tieline with midpoint load.

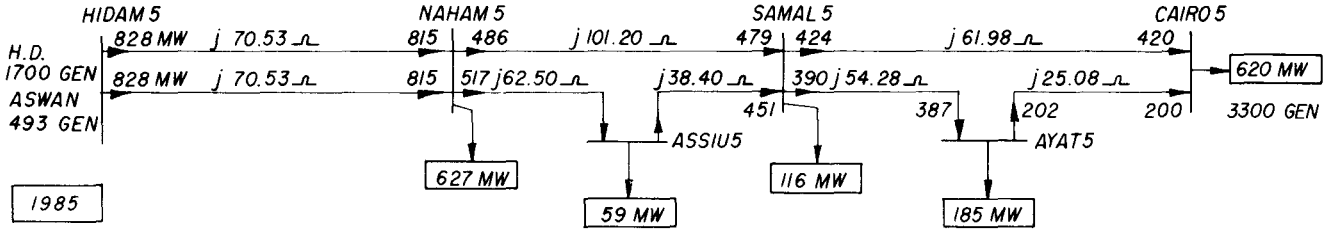

TOTAL SYSTEM GENERATION = 5985 MW

Figure 7. – 500-kV power system.

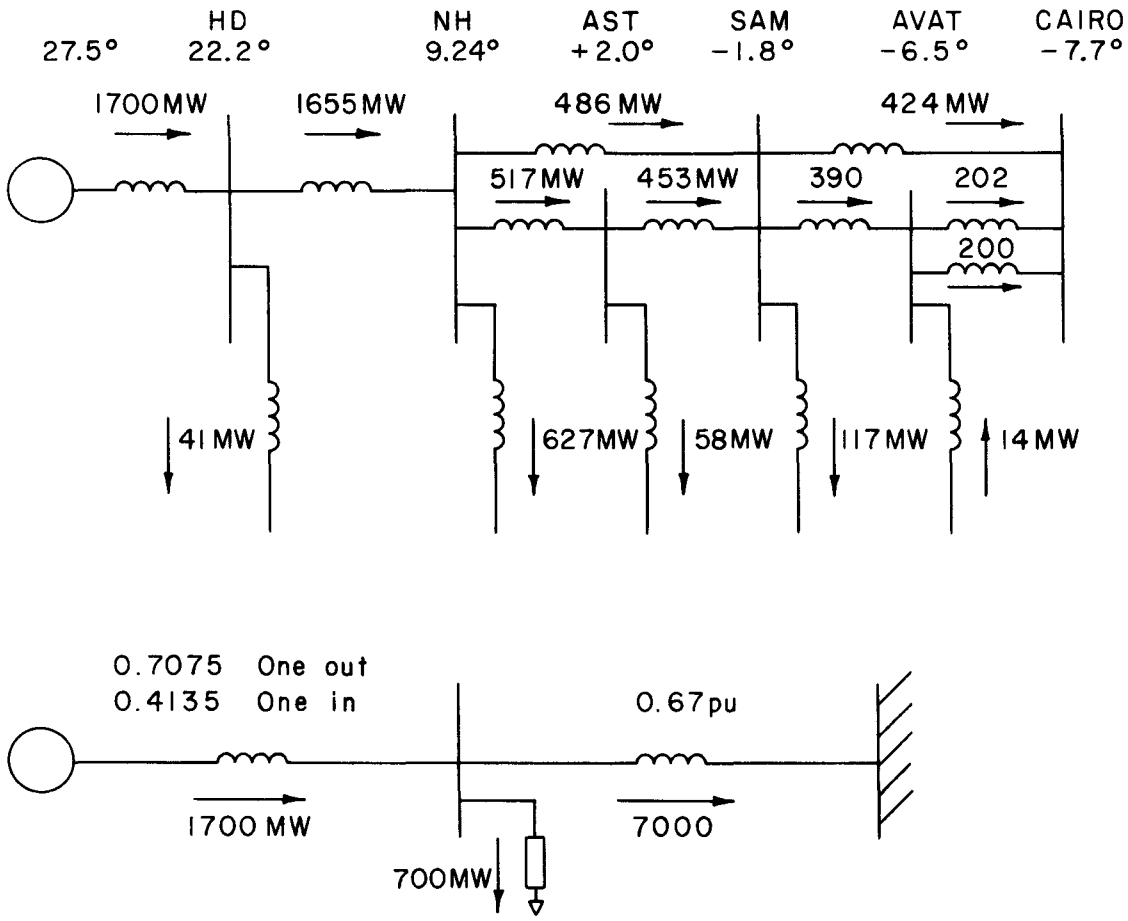

HD ⟶ NH 0.4135pu Both lines in

0.7075pu One line out

NH ⟶ CAIRO 0.67pu

Load at NH ⟶ ≈ 700 MW ⟶ 0.34pu

Power to Cairo ⟶ ≈ 1000MW ⟶ 0.485pu

Total Generation 1700MW ⟶ 0.825pu

Figure 8. – Model of modified 500-kV power system.

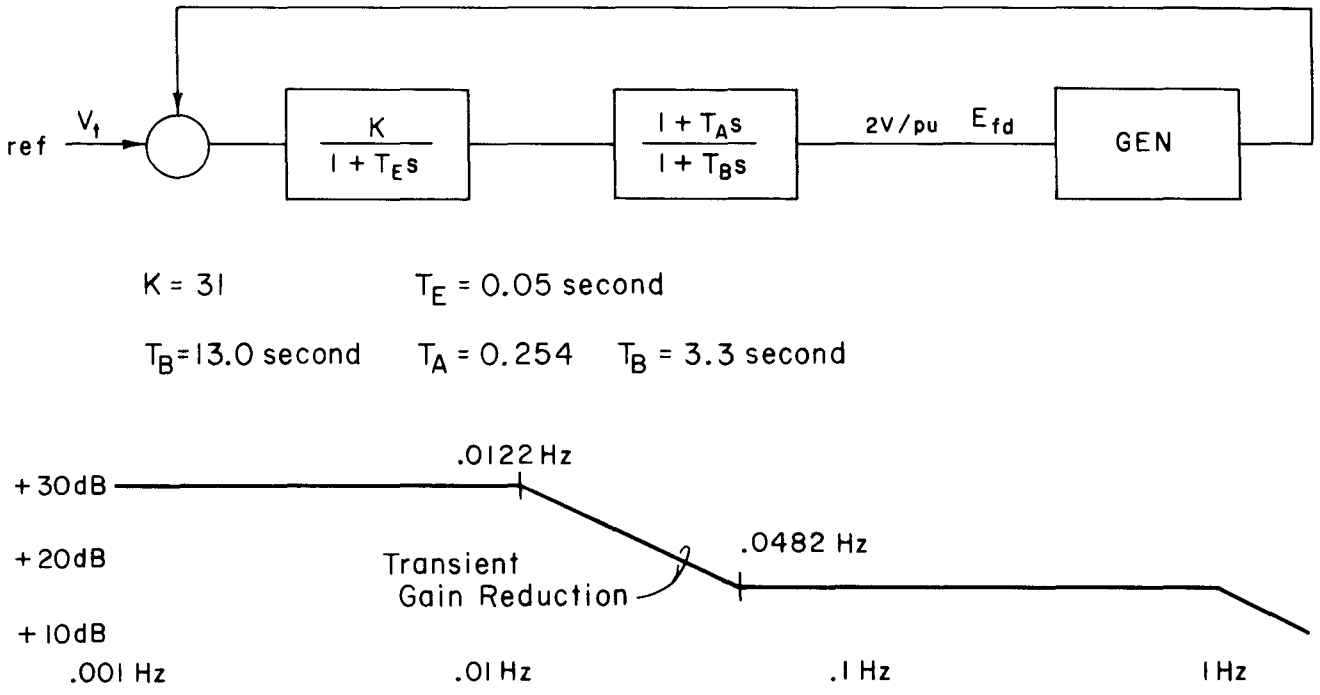

Figure 9. – IEEE Type AC4 regulator model.

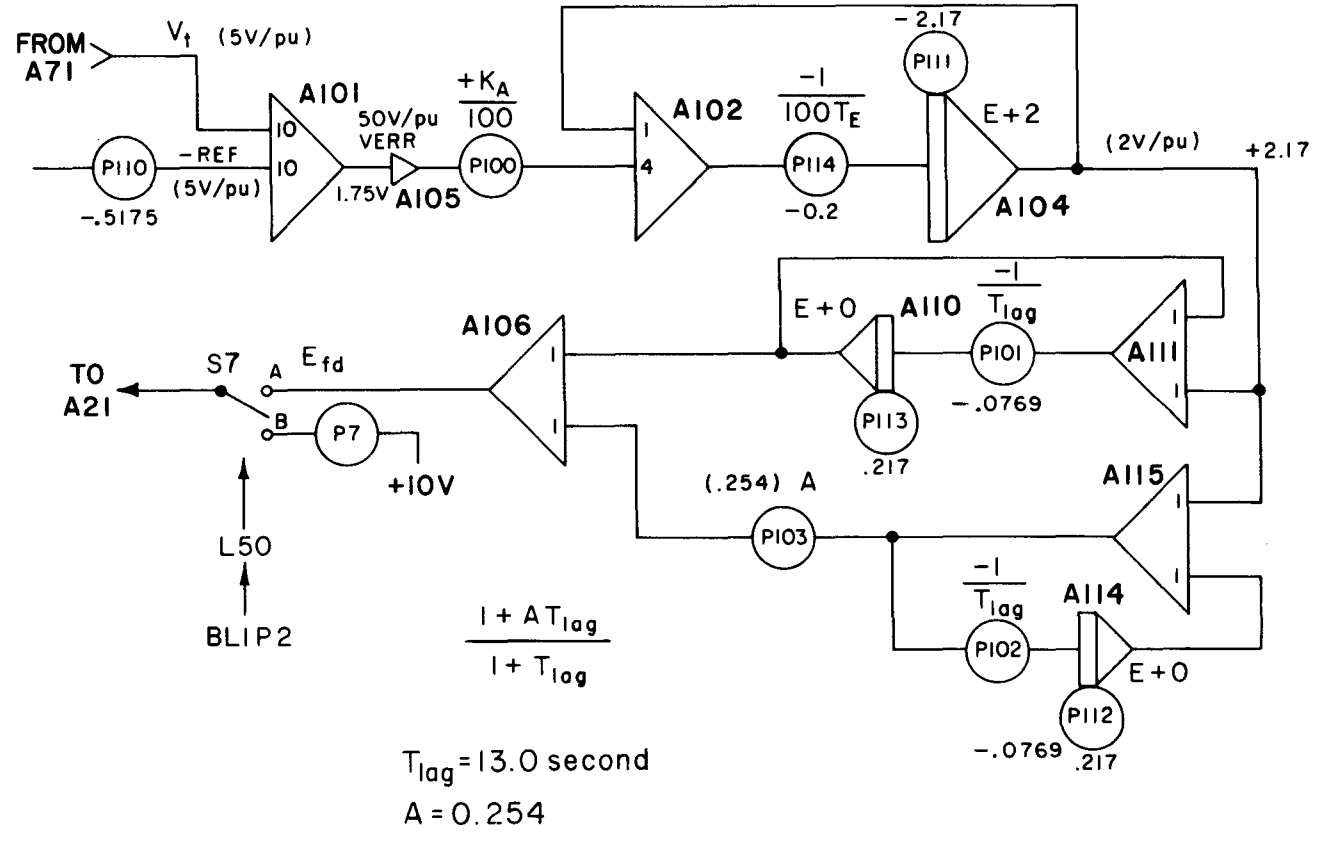

Figure 10. – IEEE Type AC4 regulator analog computer diagram.

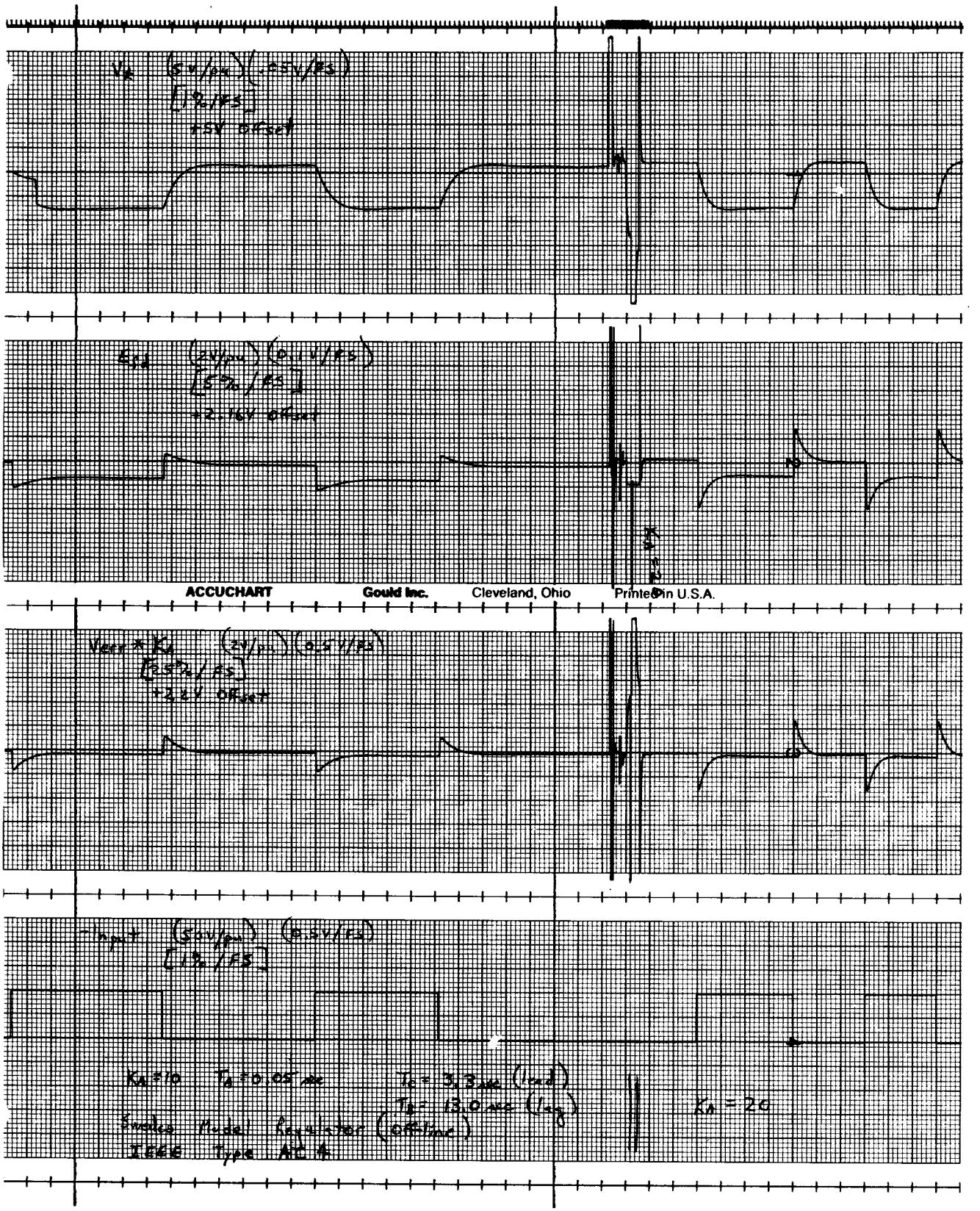

Figure 11. – Off-line time-domain responses with IEEE Type AC4 regulator (sheet 1 of 4).

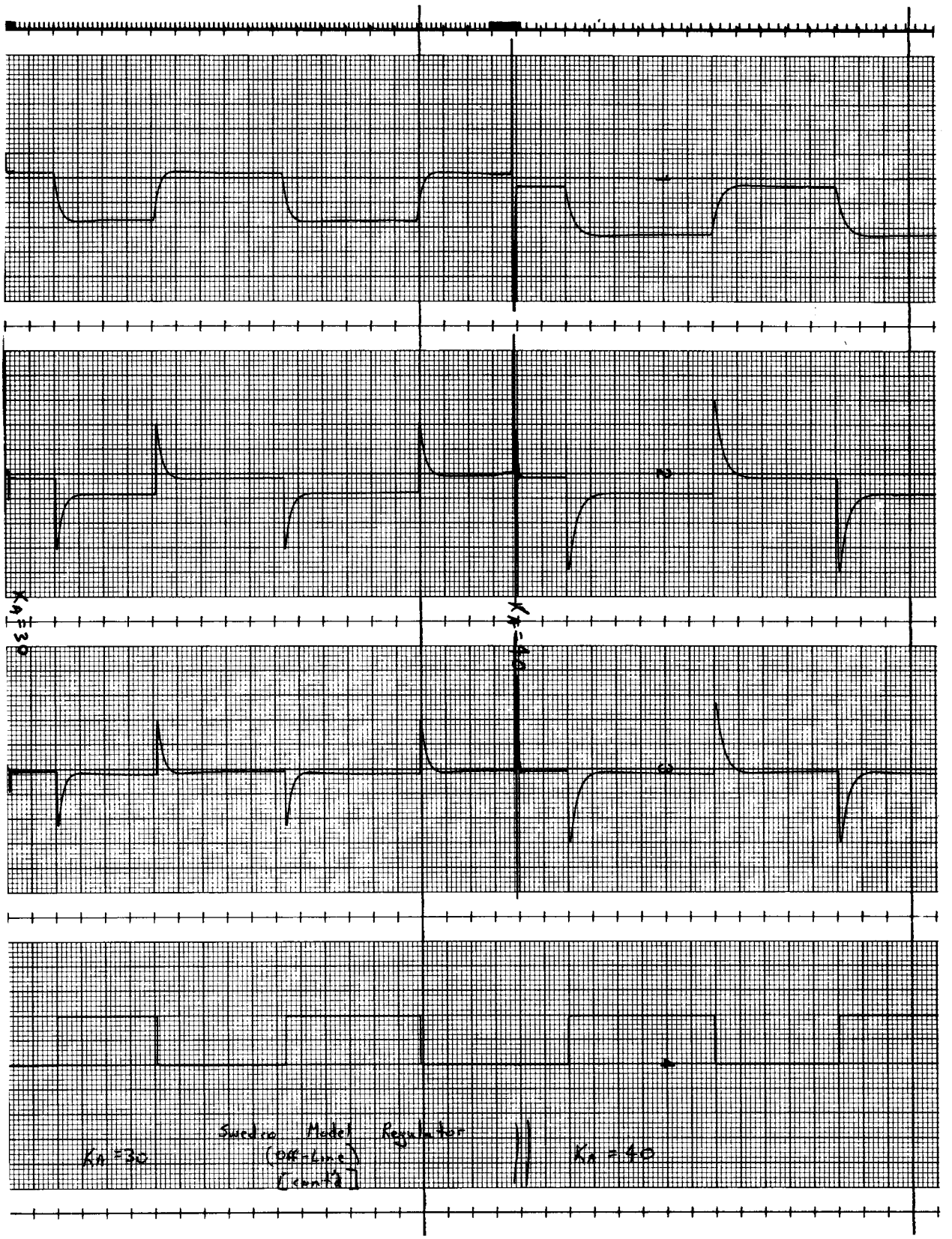

Figure 11. – Off-line time-domain responses with IEEE Type AC4 regulator (sheet 2 of 4).

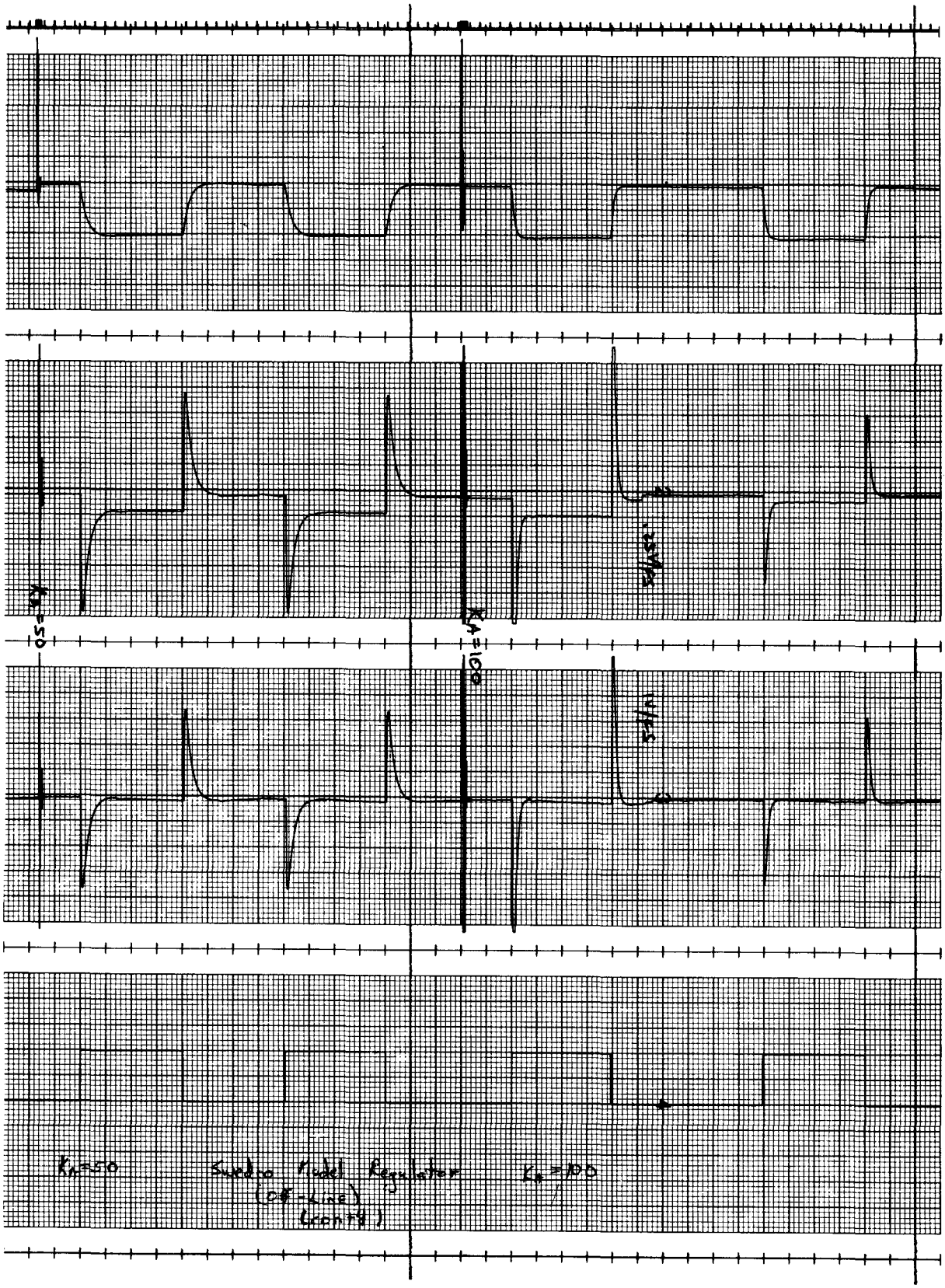

Figure 11. – Off-line time-domain responses with IEEE Type AC4 regulator (sheet 3 of 4).

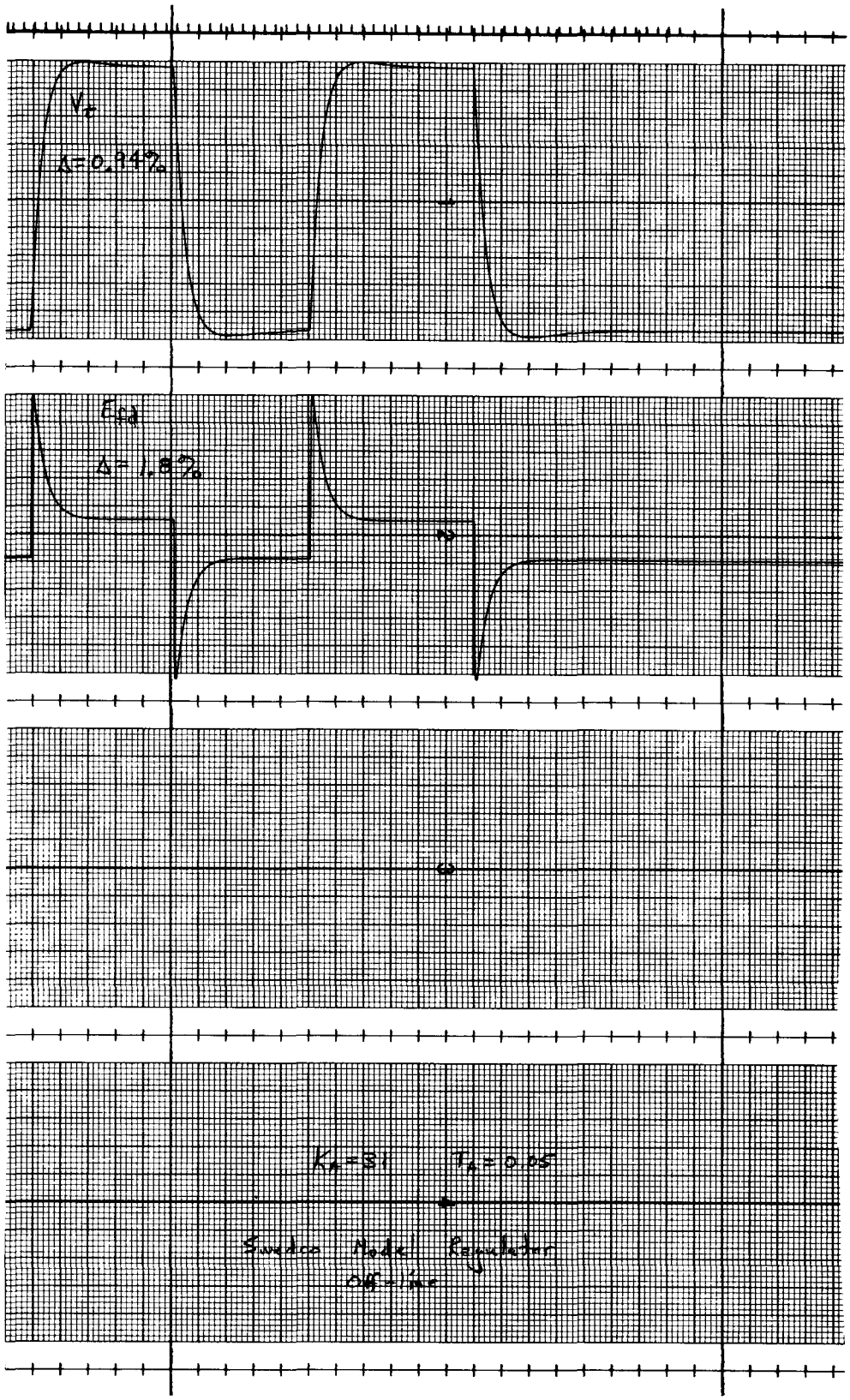

Figure 11. – Off-line time-domain responses with IEEE Type AC4 regulator (sheet 4 of 4).

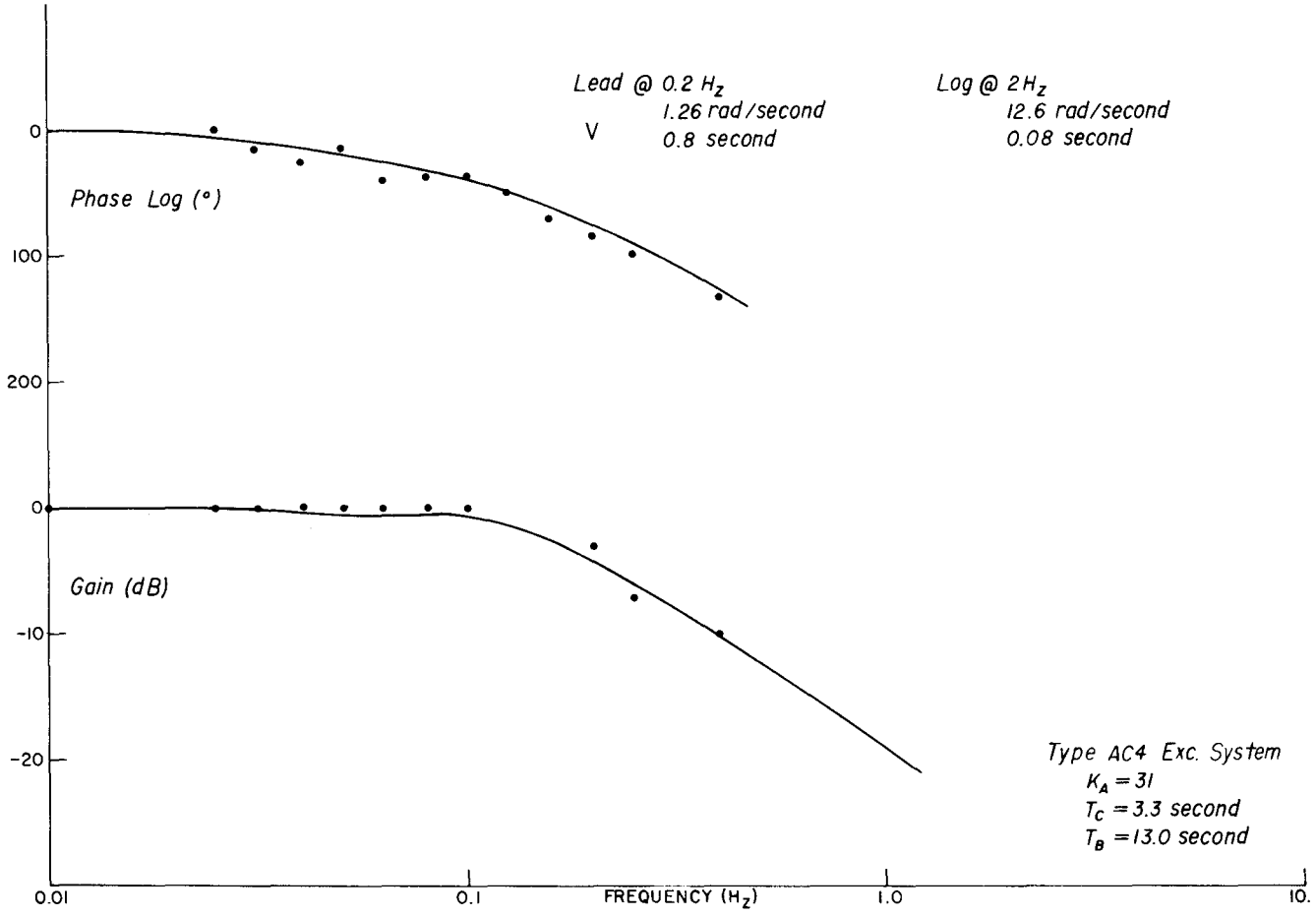

Figure 12. – Off-line frequency response with IEEE Type AC4 regulator.

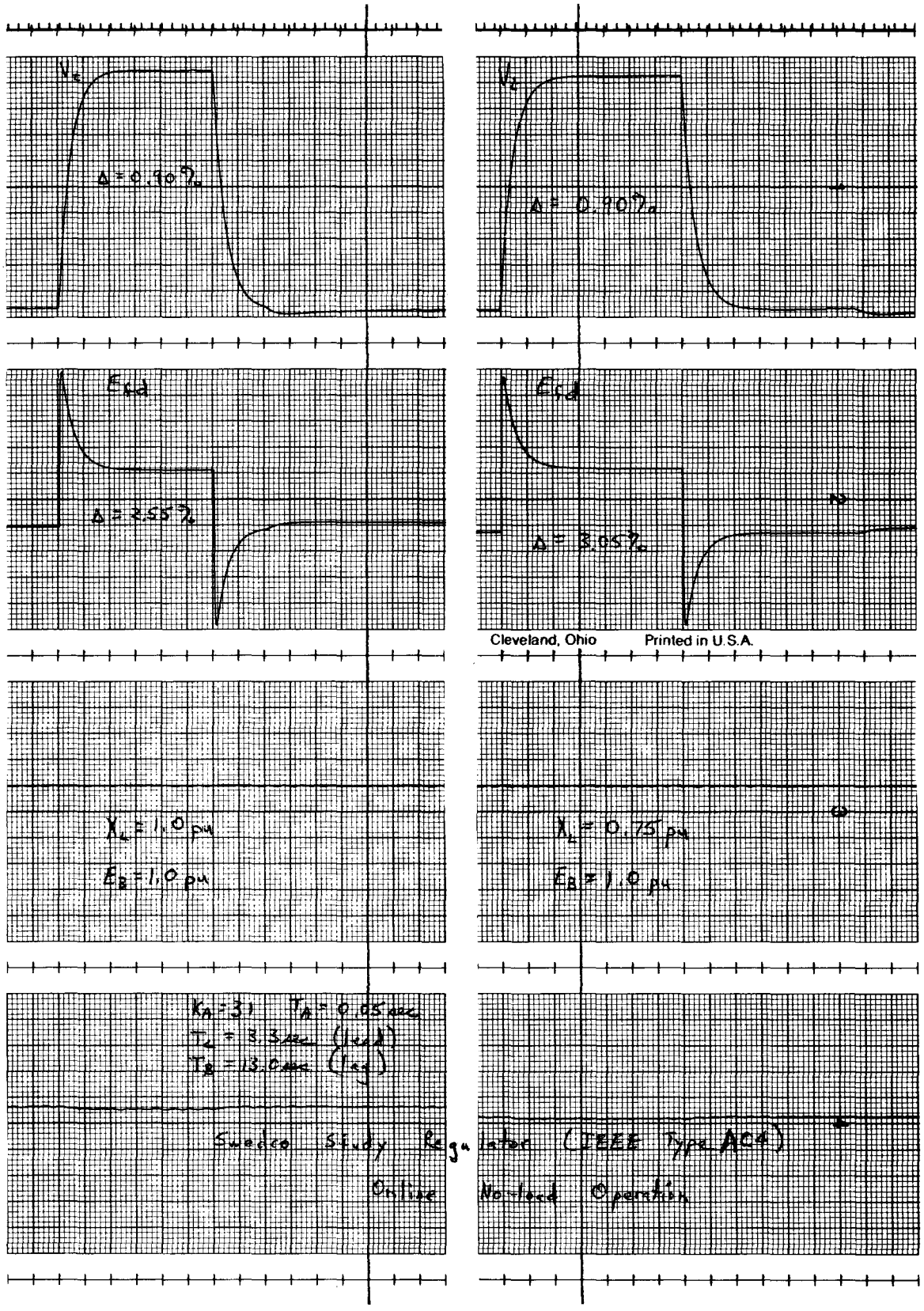

Figure 13. – On-line time-domain responses with IEEE Type AC4 regulator (sheet 1 of 5).

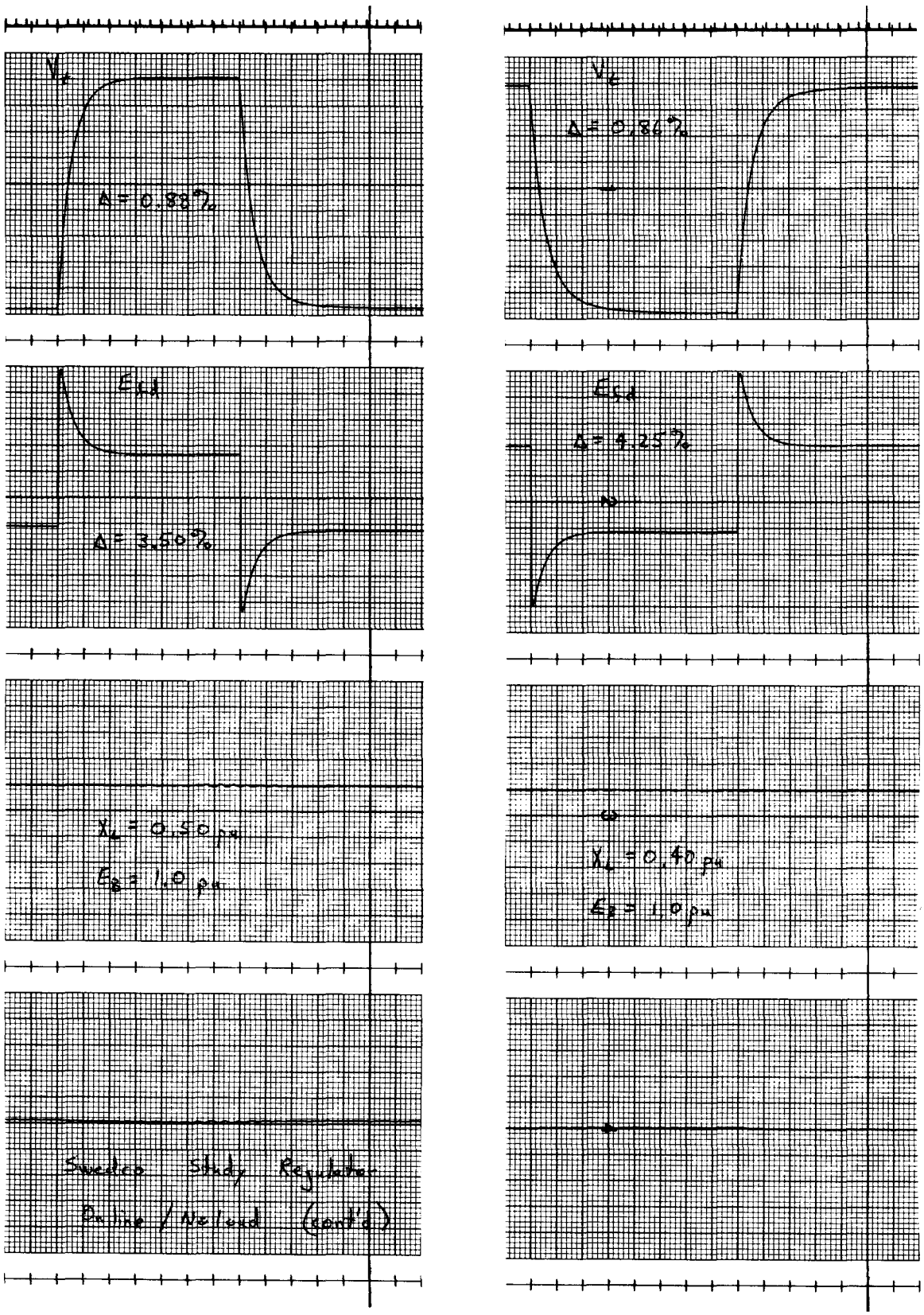

Figure 13. – On-line time-domain responses with IEEE Type AC4 regulator (sheet 2 of 5).

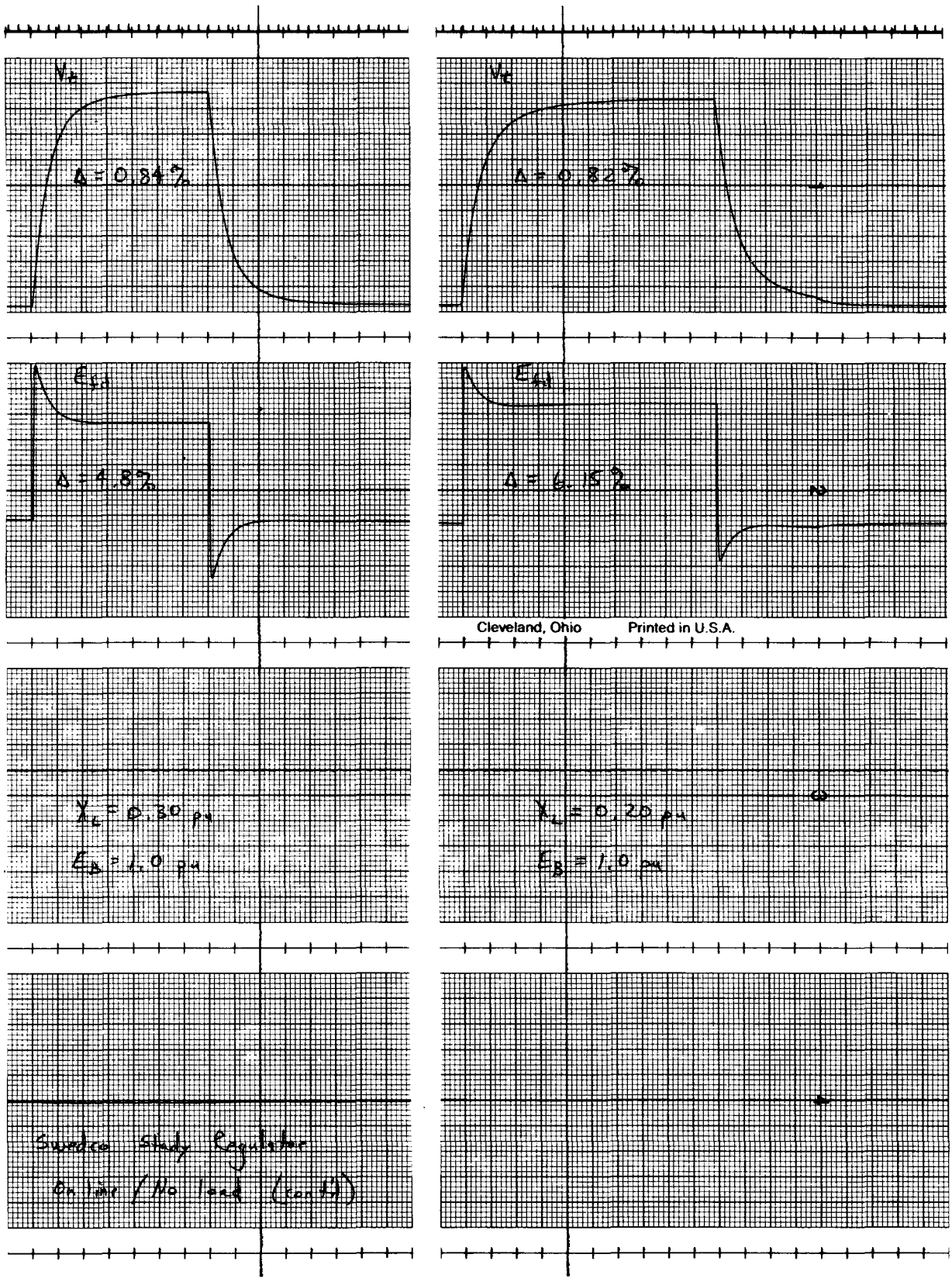

Figure 13. – On-line time-domain responses with IEEE Type AC4 regulator (sheet 3 of 5).

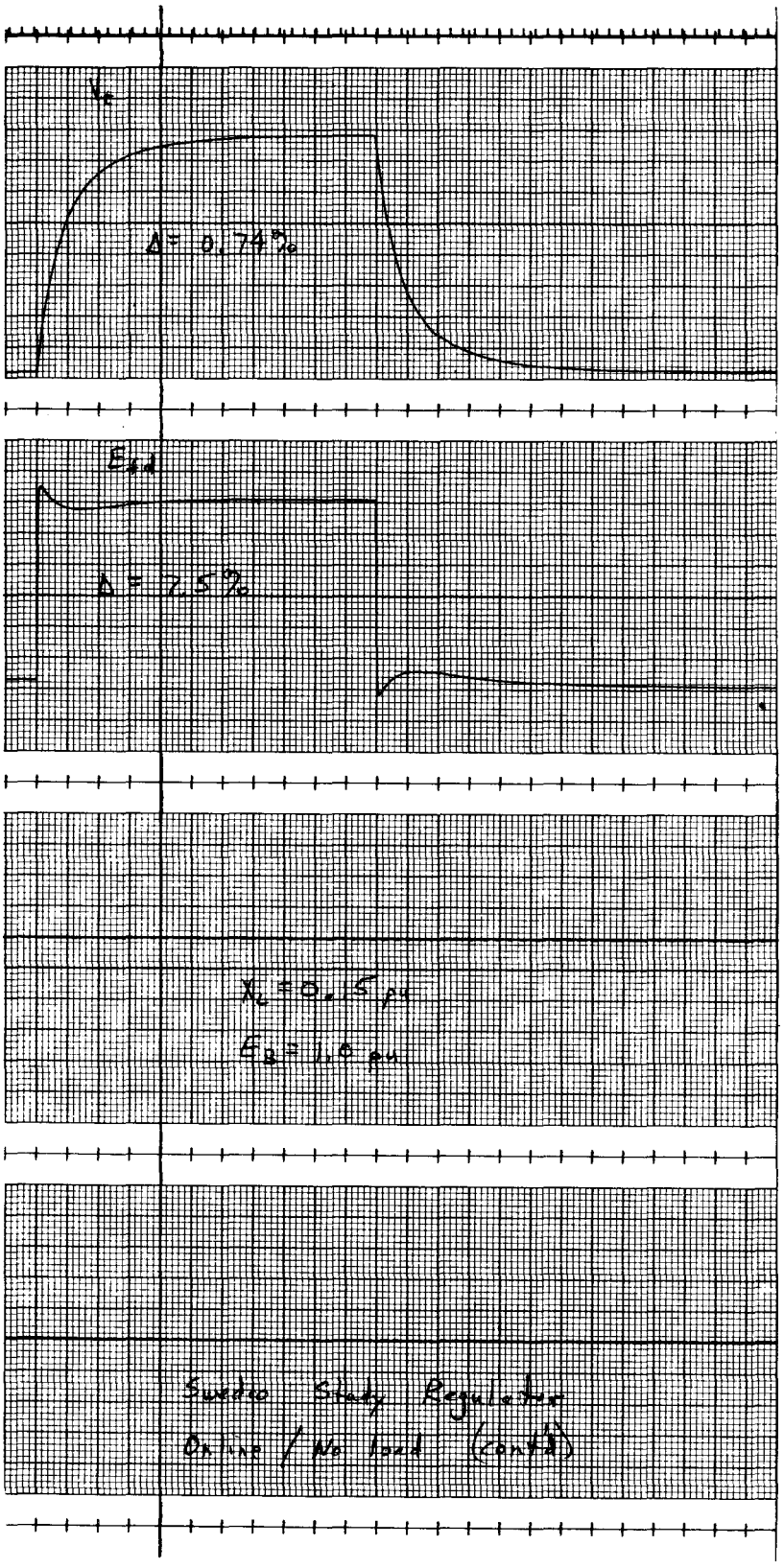

Figure 13. – On-line time-domain responses with IEEE Type AC4 regulator (sheet 4 of 5).

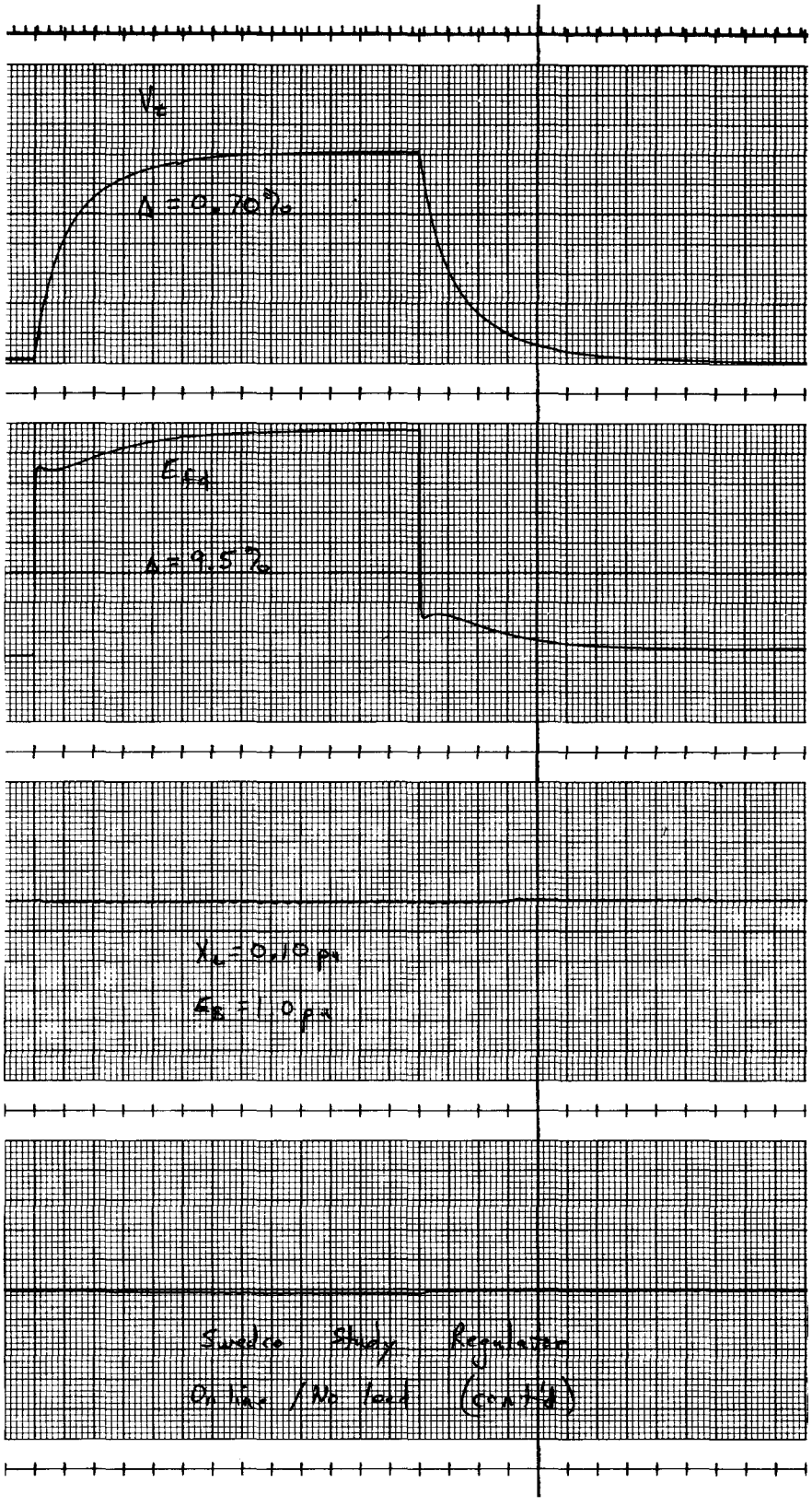

Figure 13. – On-line time-domain responses with IEEE Type AC4 regulator (sheet 5 of 5).

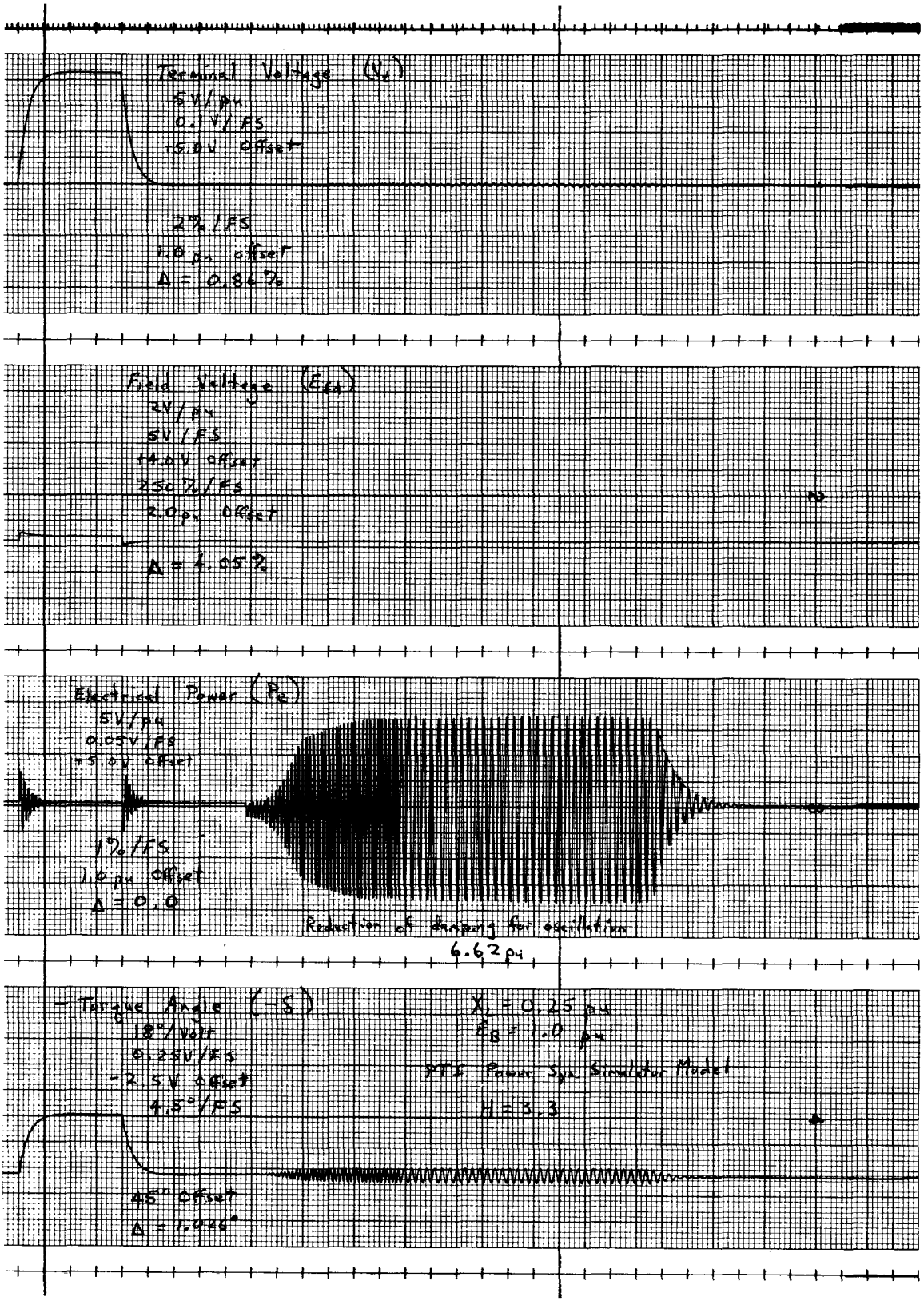

Figure 14. – System performance for various values of line impedance and damping (sheet 1 of 8).

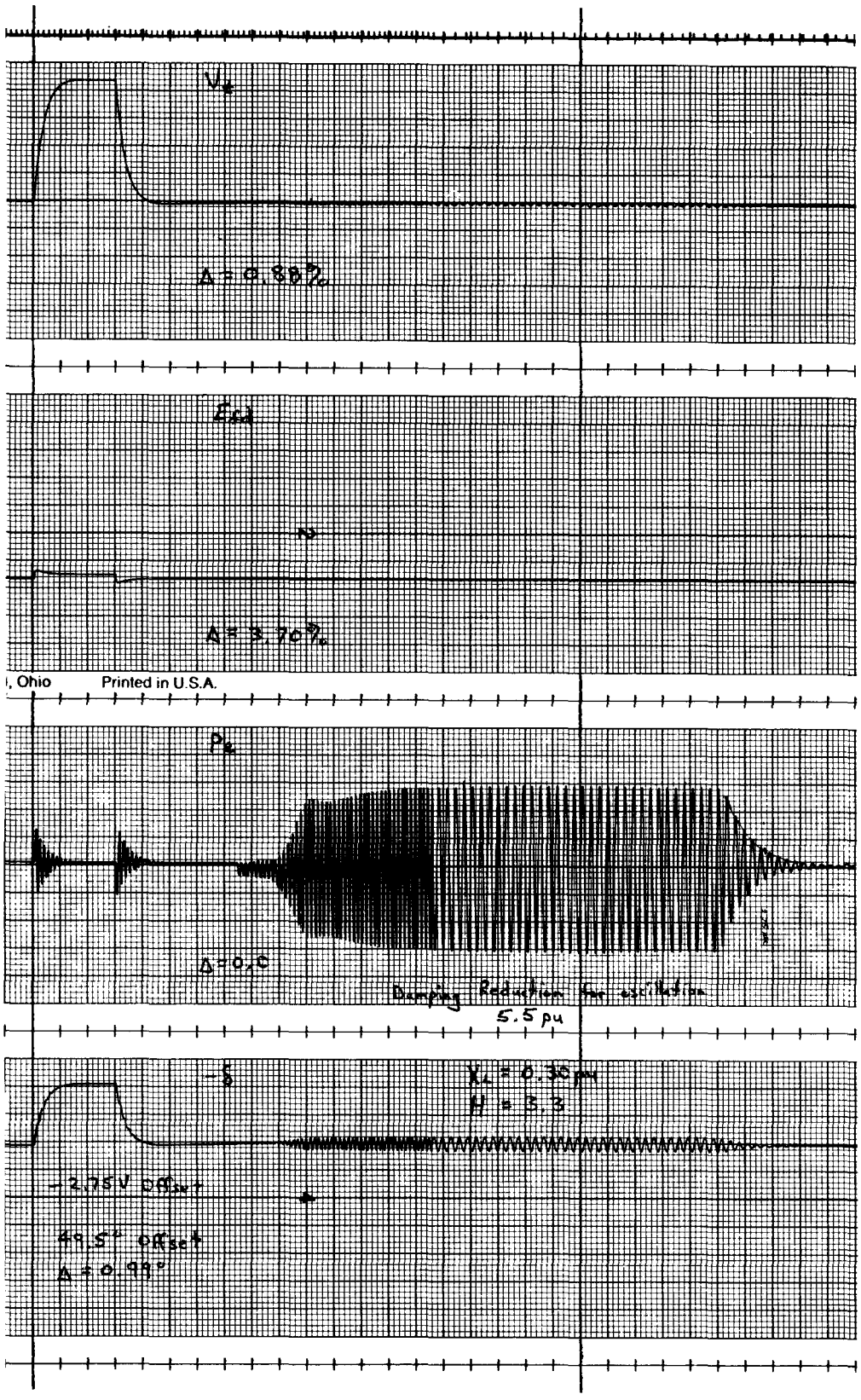

Figure 14. – System performance for various values of line impedance and damping (sheet 2 of 8).

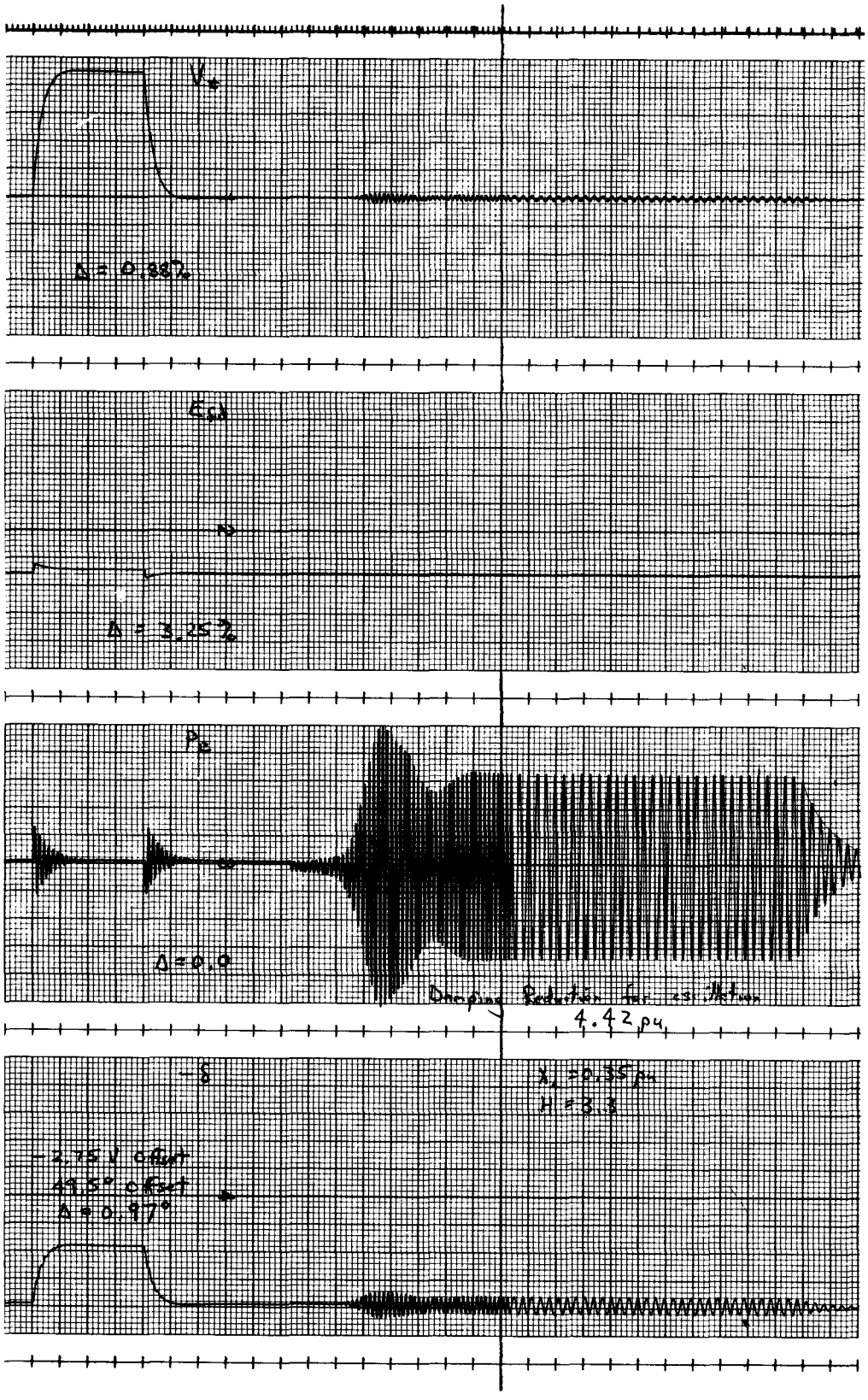

Figure 14. – System performance for various values of line impedance and damping (sheet 3 of 8).

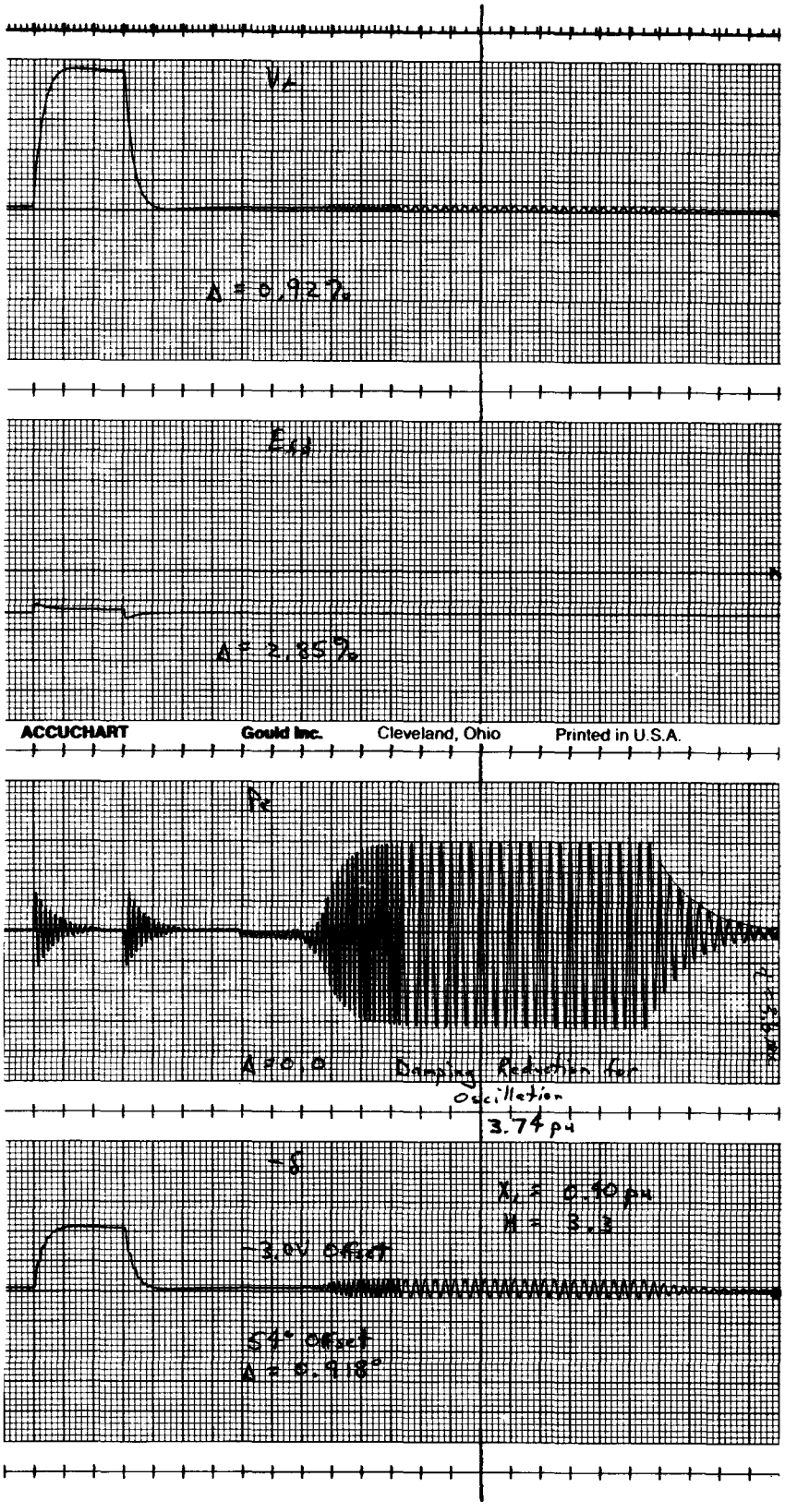

Figure 14. – System performance for various values of line impedance and damping (sheet 4 of 8).

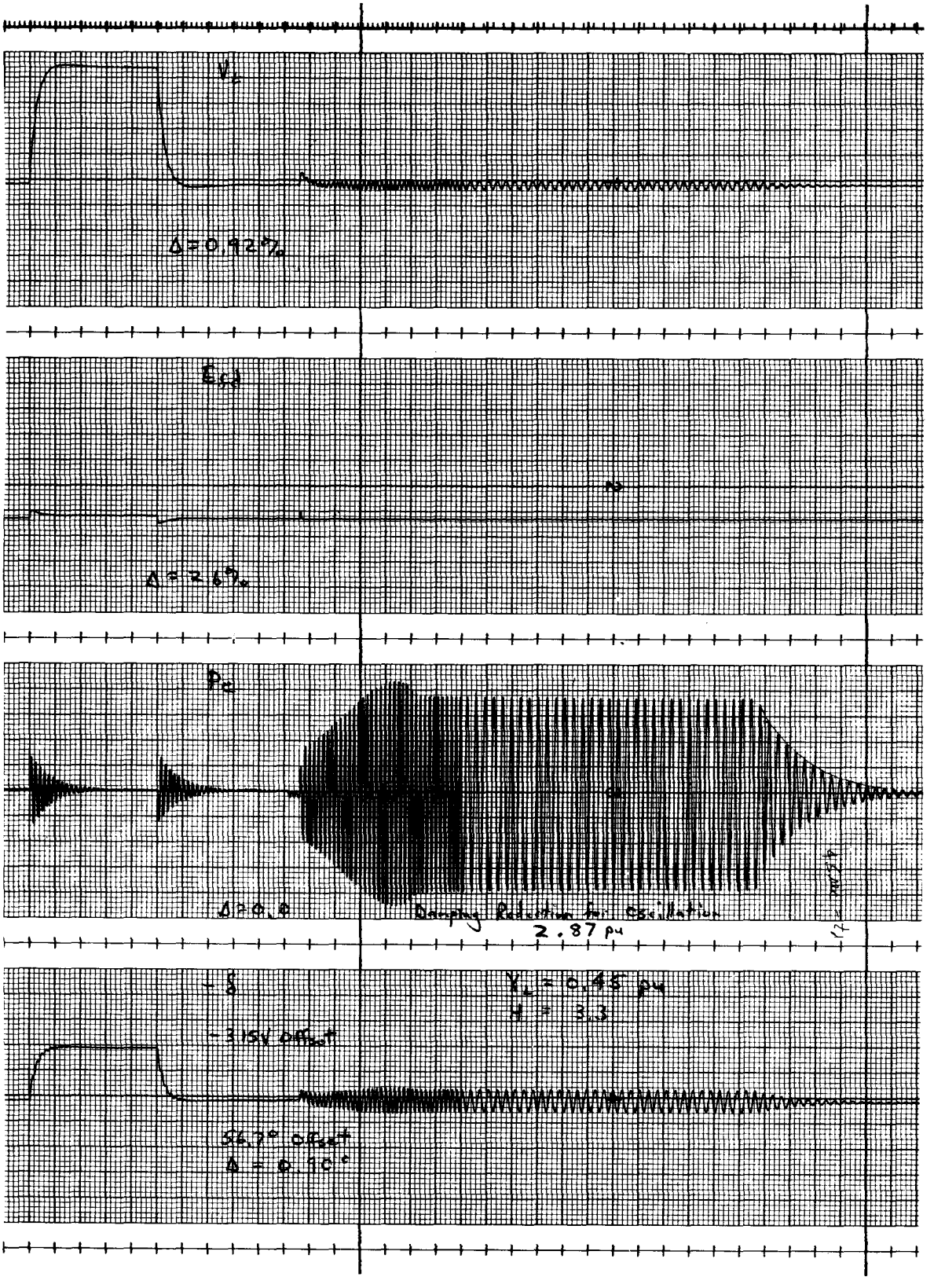

Figure 14. – System performance for various values of line impedance and damping (sheet 5 of 8).

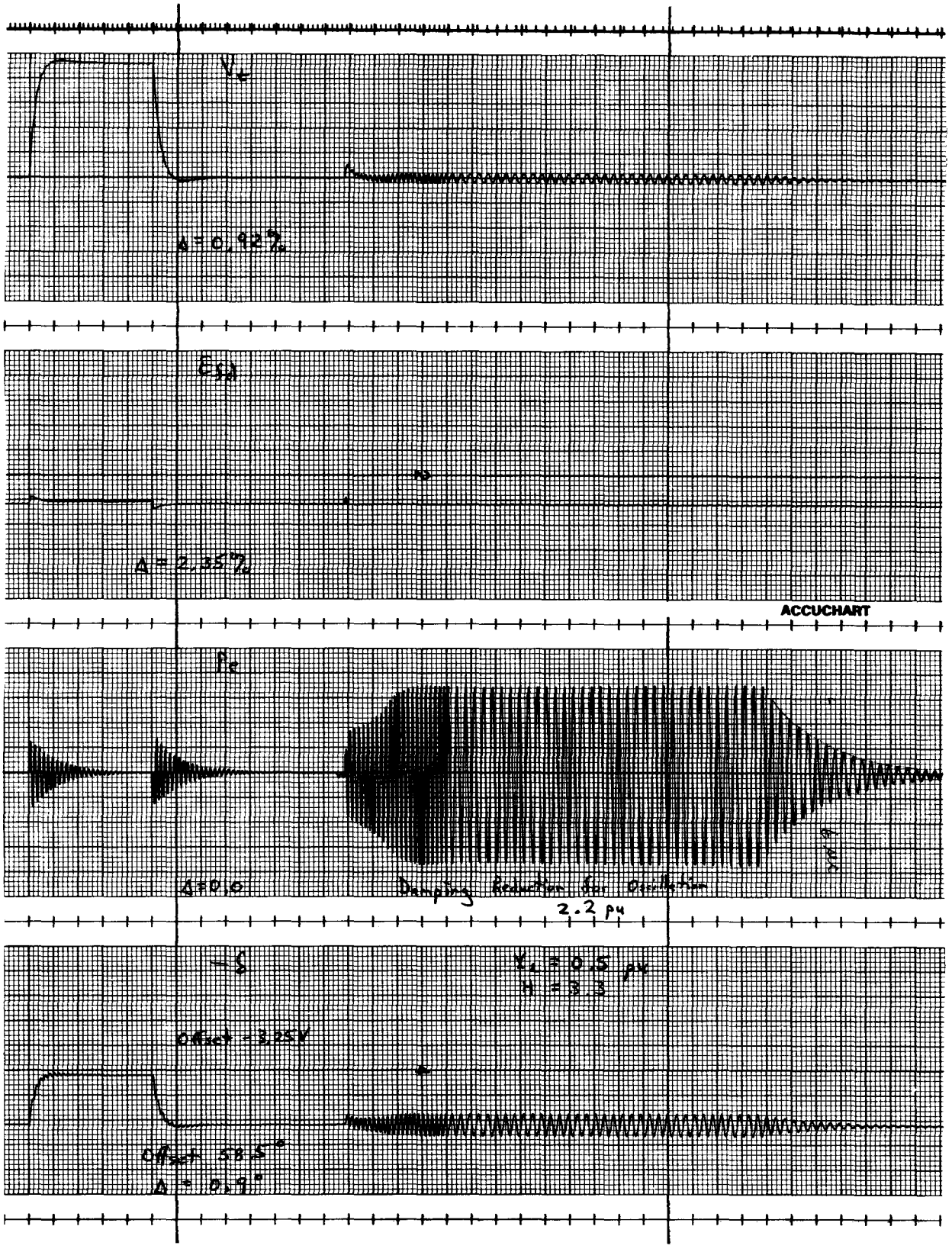

Figure 14. – System performance for various values of line impedance and damping (sheet 6 of 8).

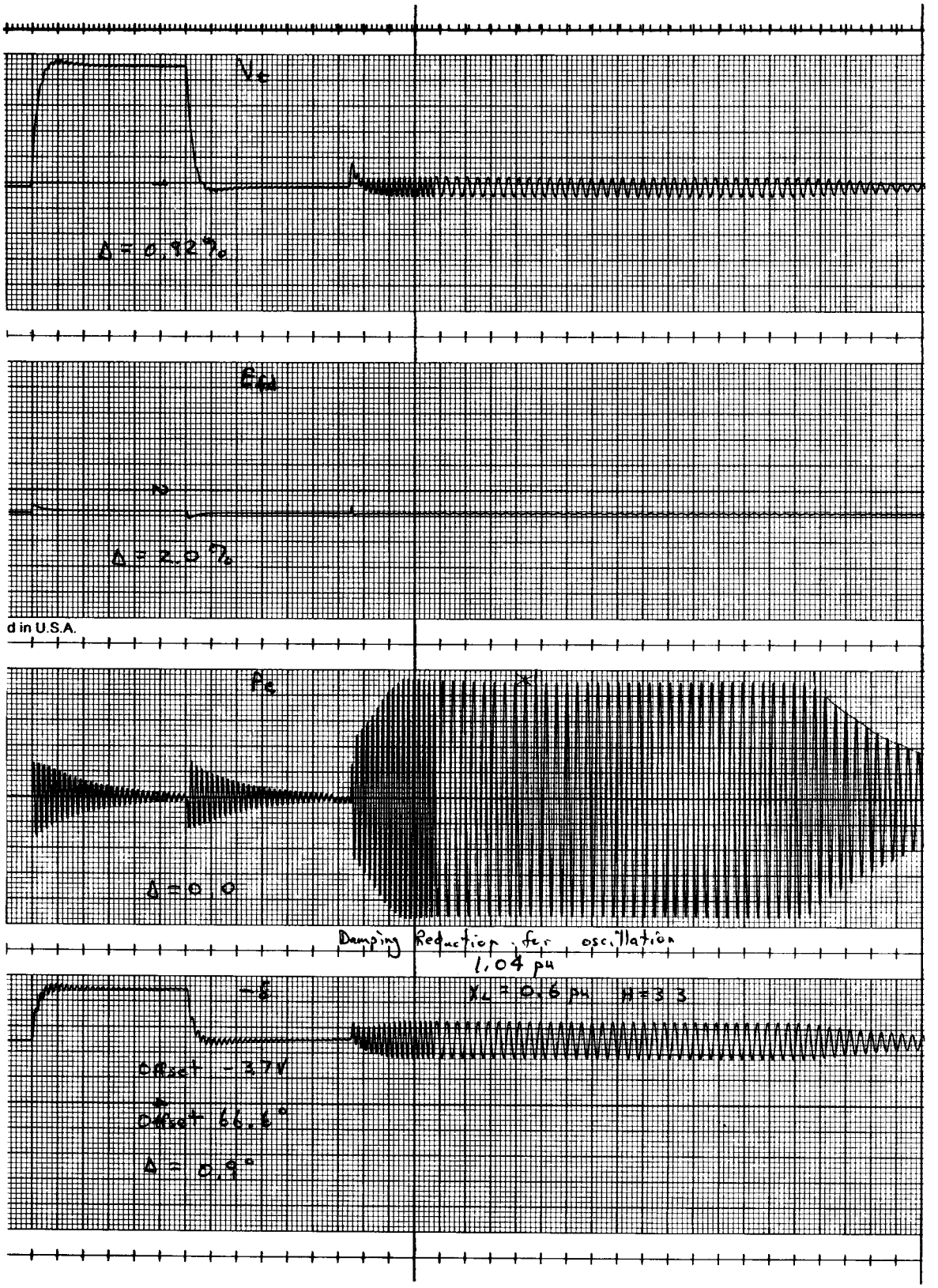

Figure 14. – System performance for various values of line impedance and damping (sheet 7 of 8).

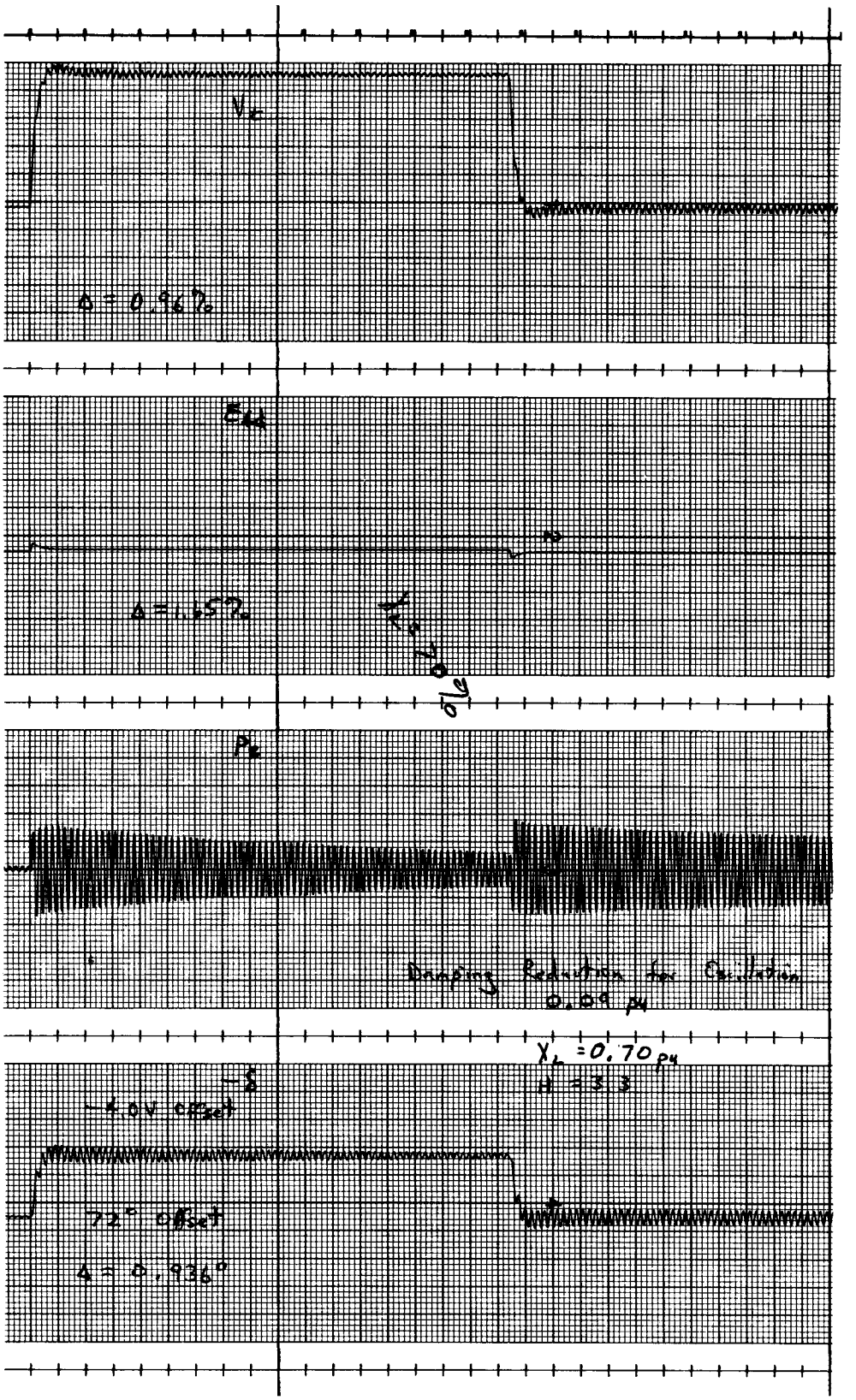

Figure 14. – System performance for various values of line impedance and damping (sheet 8 of 8).

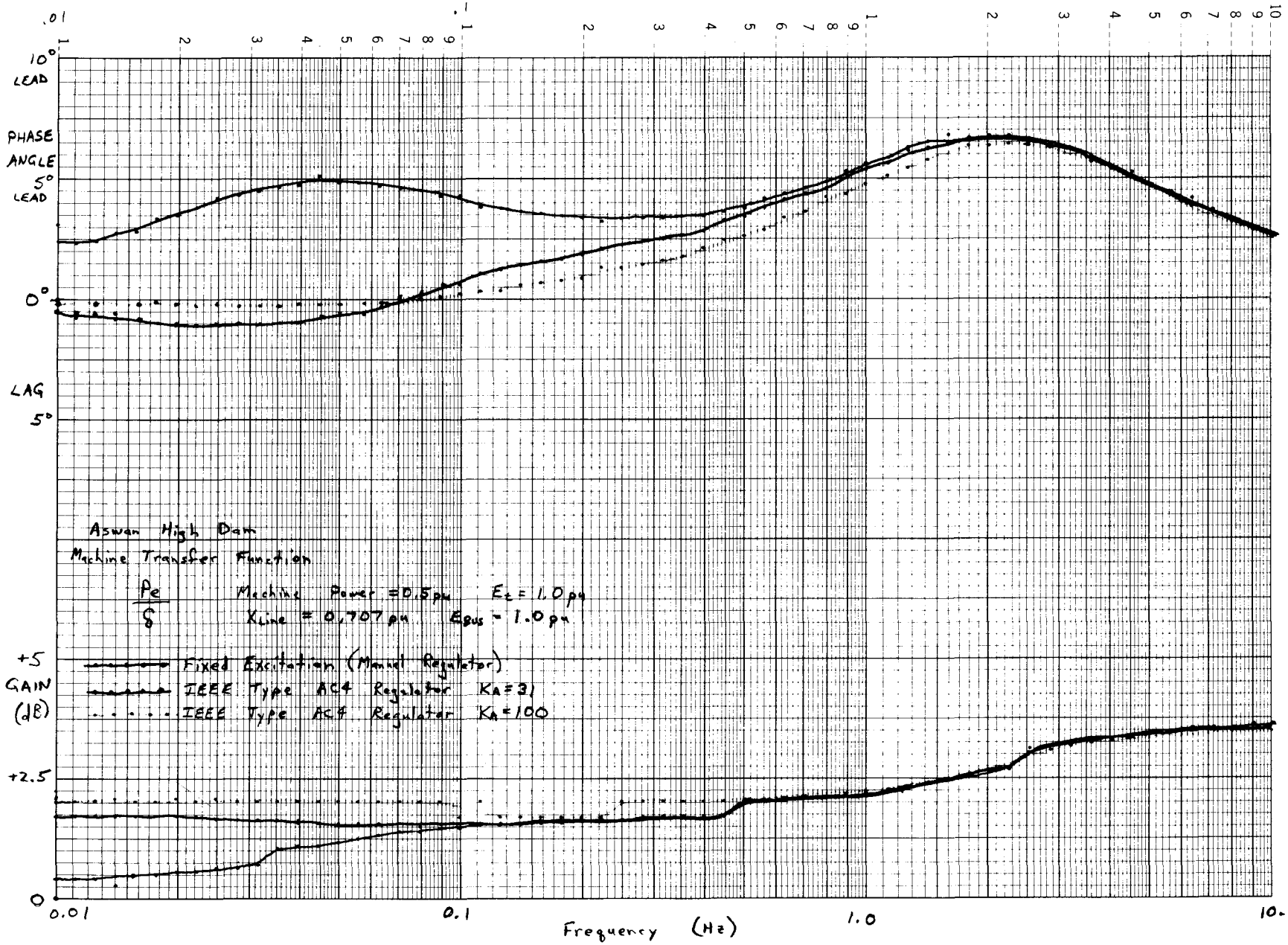

Figure 15. – Bode plots of the machine transfer function (sheet 1 of 3).

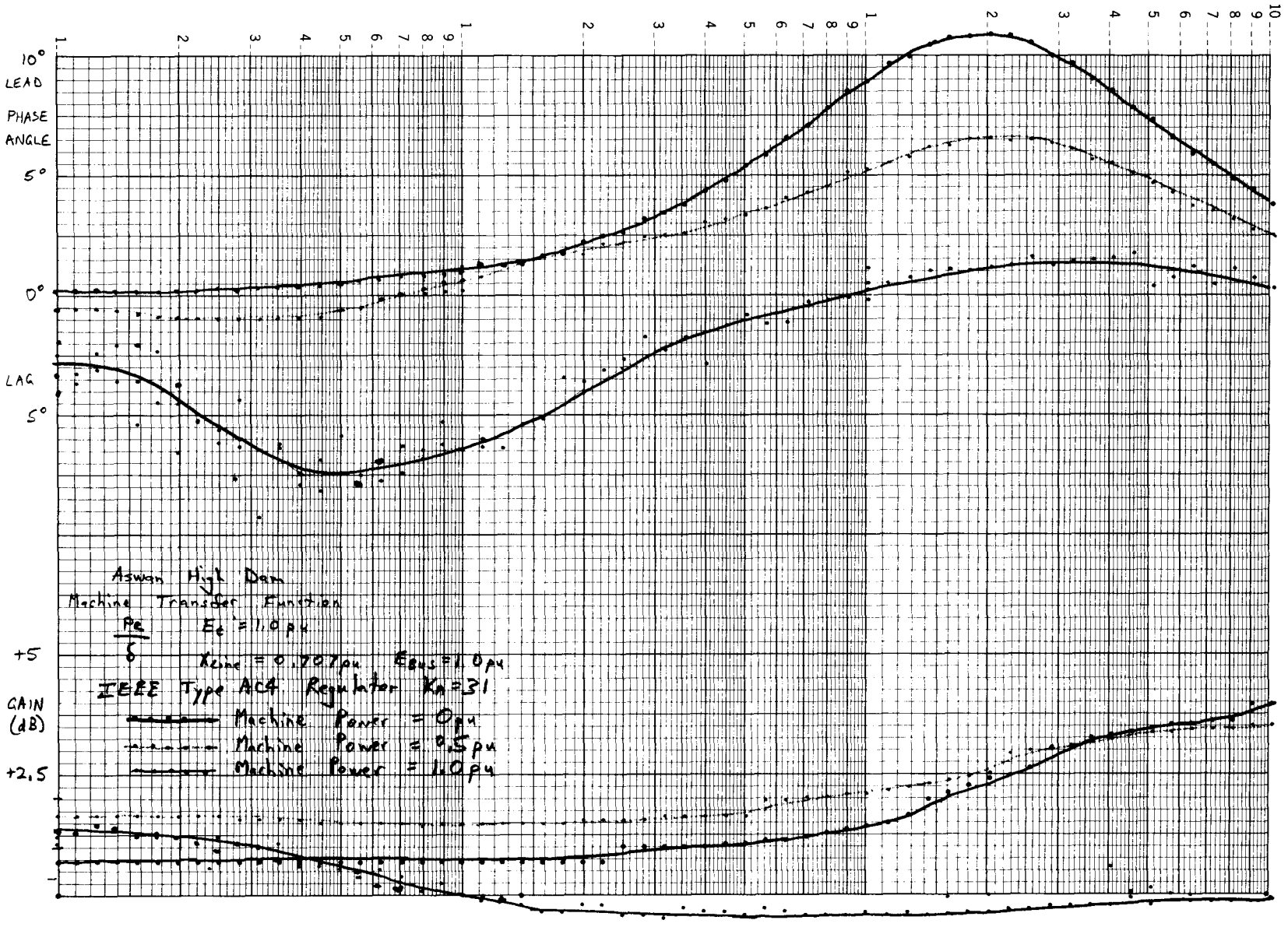

Figure 15. – Bode plots of the machine transfer function (sheet 2 of 3).

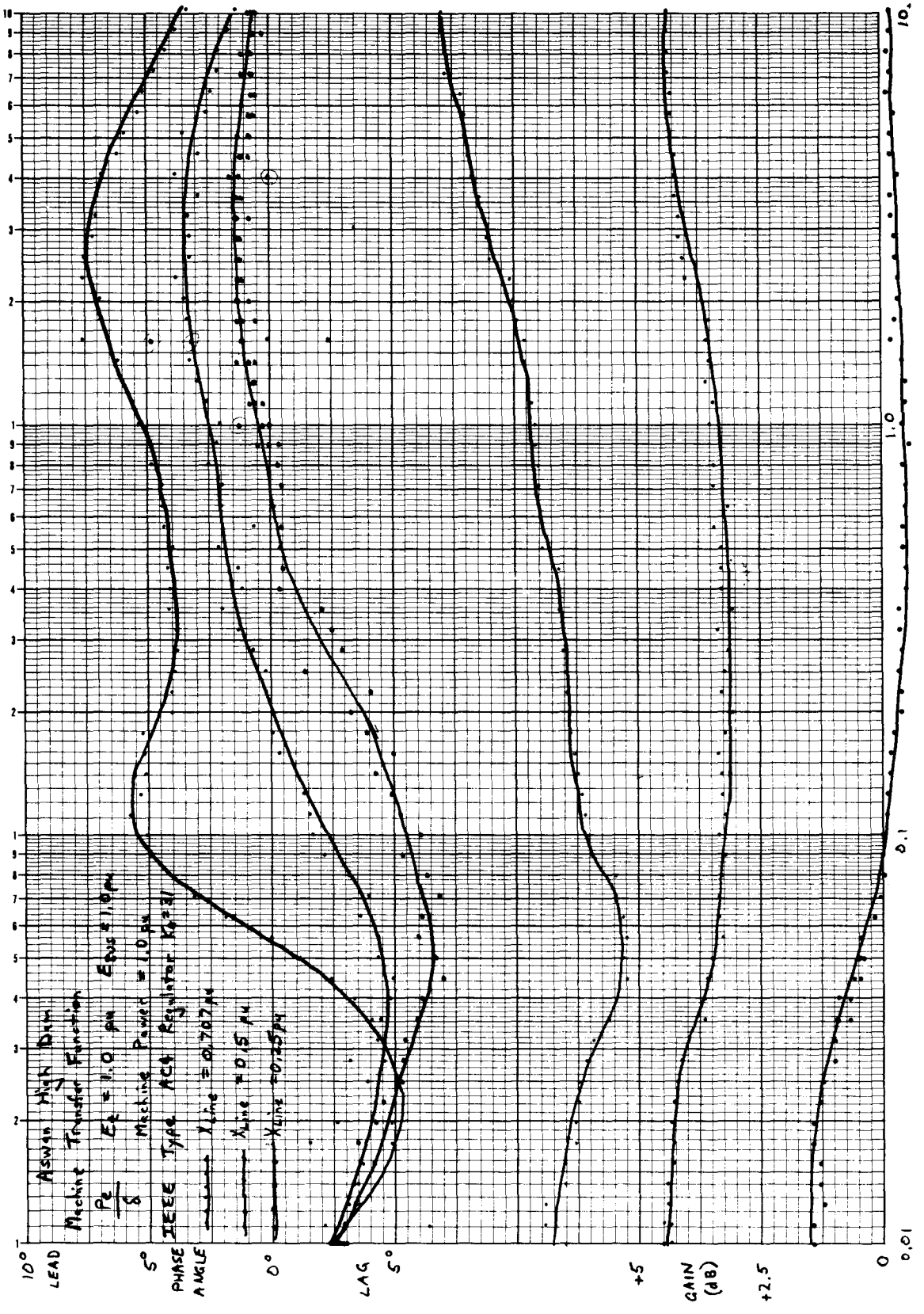

Figure 15. – Bode plots of the machine transfer function (sheet 3 of 3).

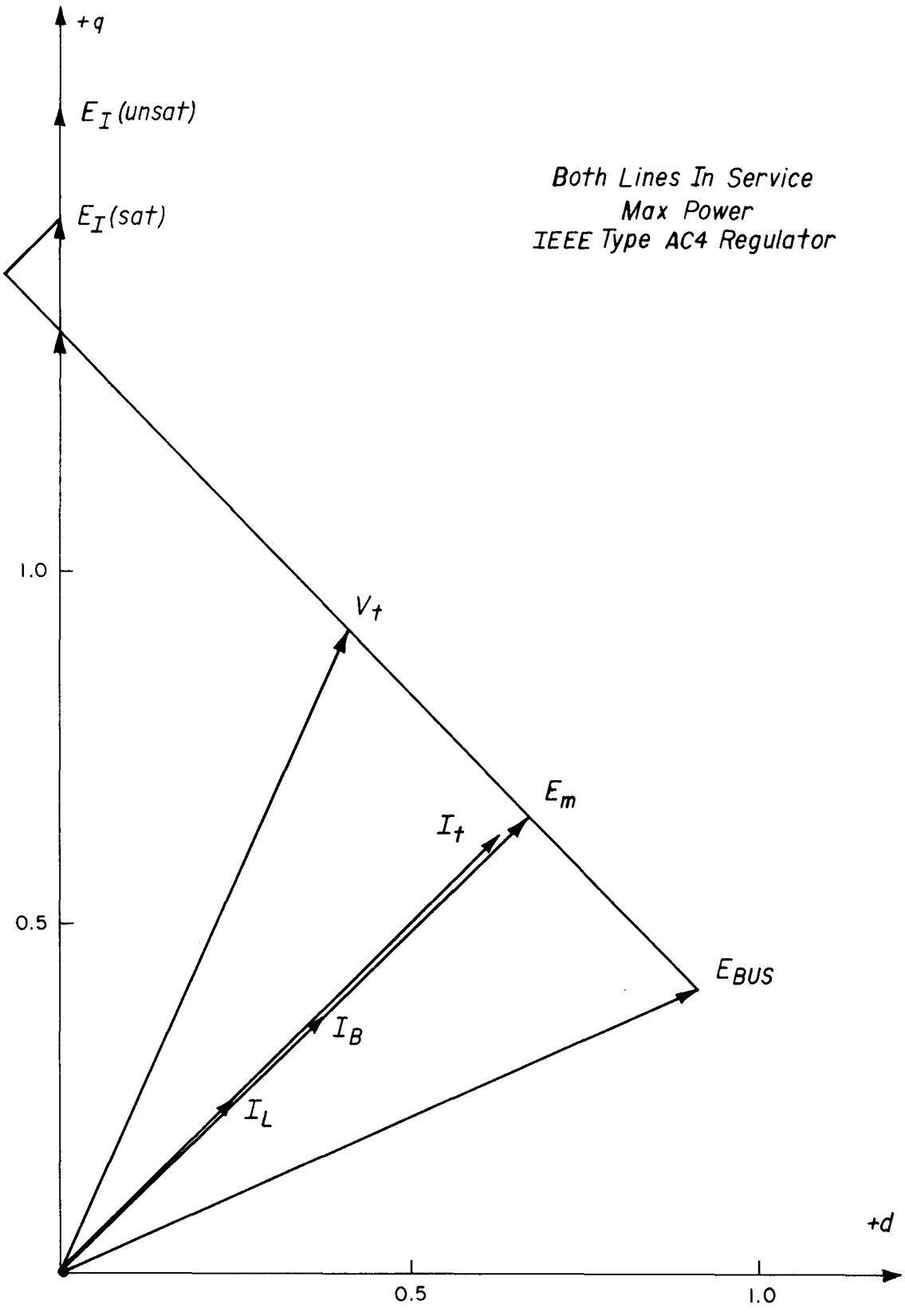

Figure 16. – Phasor diagram with both lines in service.

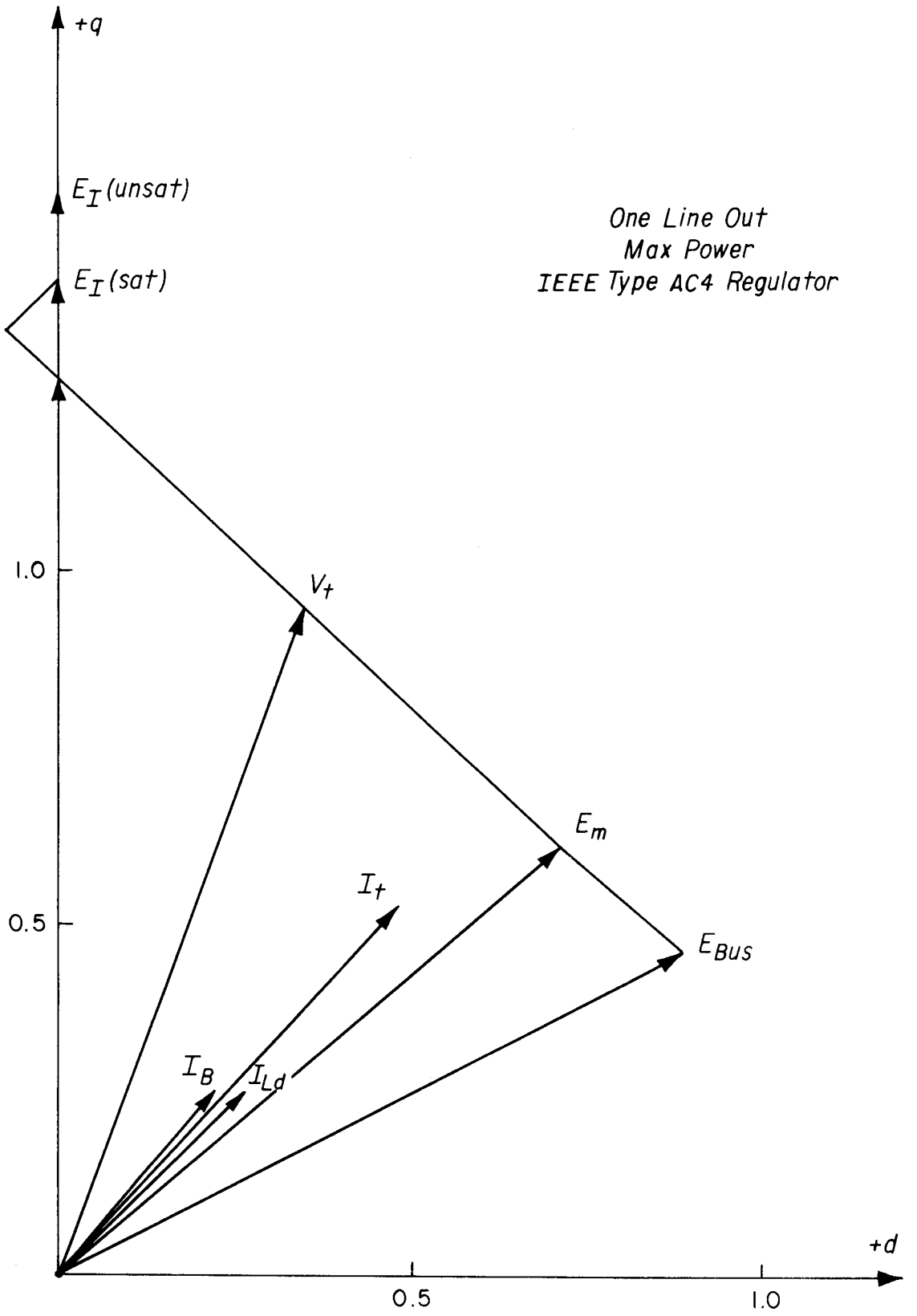

Figure 17. – Phasor diagram with only one line in service.

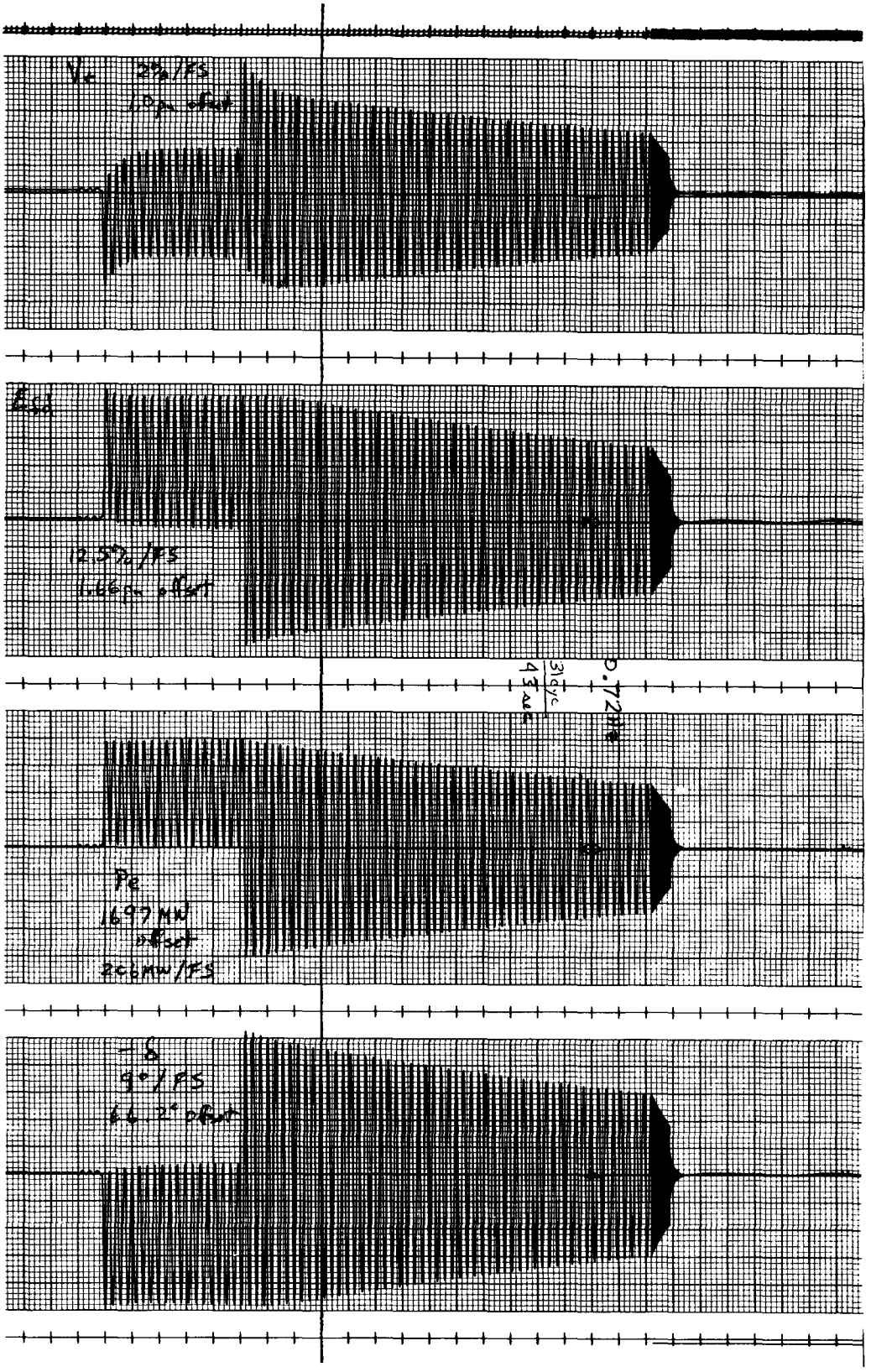

Figure 18. – System performance at full capacity with both lines in service.

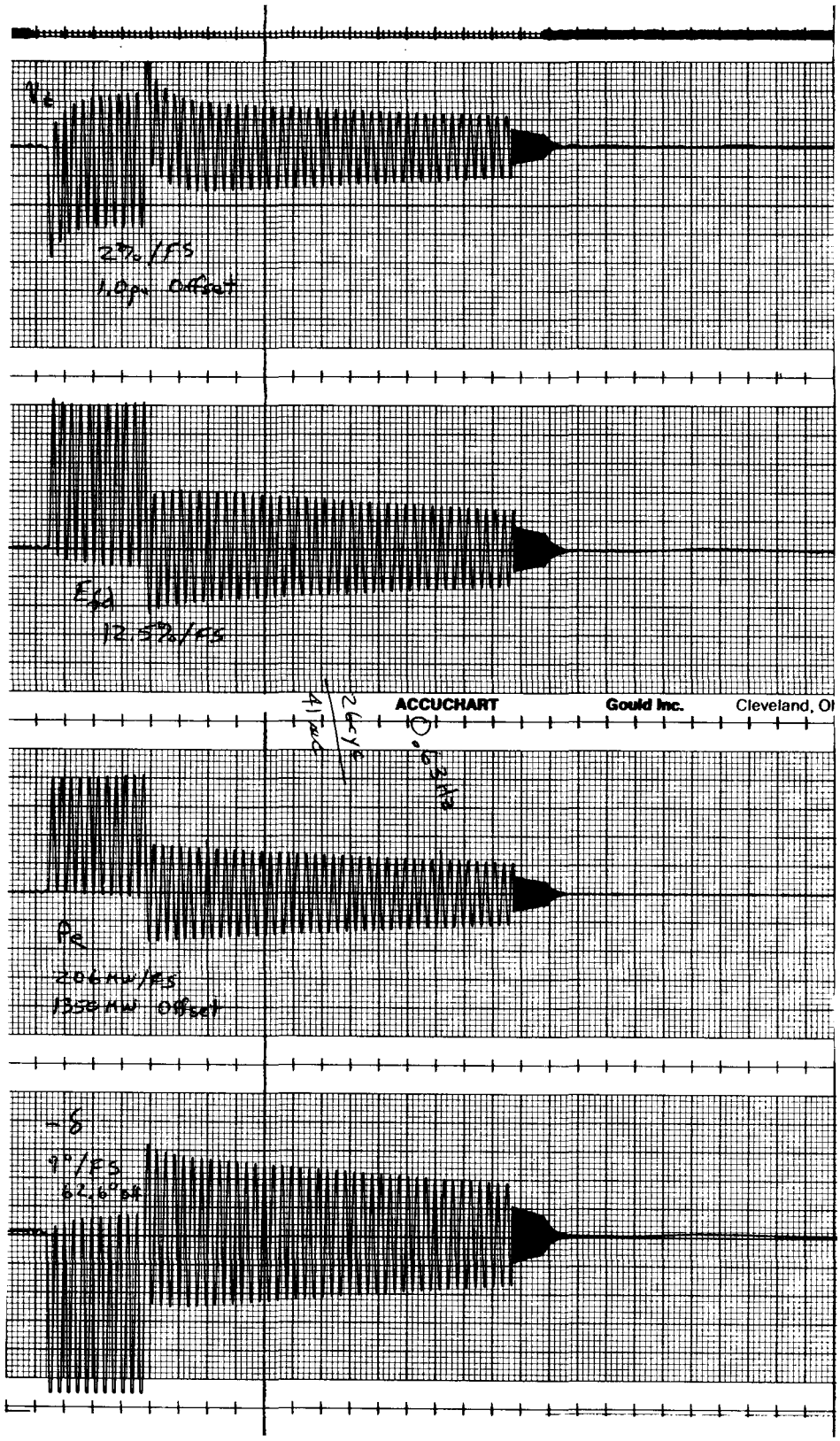

Figure 19. – System performance at full capacity with only one line in service.

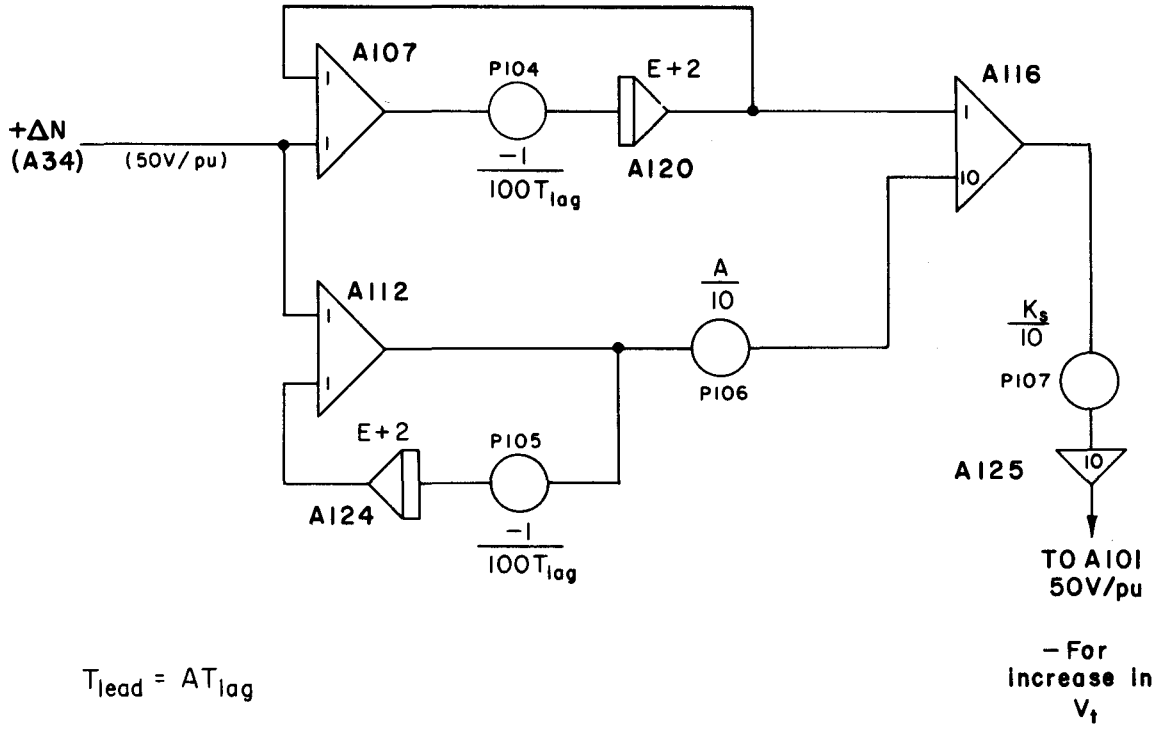

$T_{lead} = AT_{lag}$

$T_{lag} = 0.08$ second $\longrightarrow$ Pot = −0.125

$T_{lead} = 0.8$ second $= 10\,T_{lag} \longrightarrow$ Pot = 1.0

Figure 20. – Analog computer diagram of PSS function.

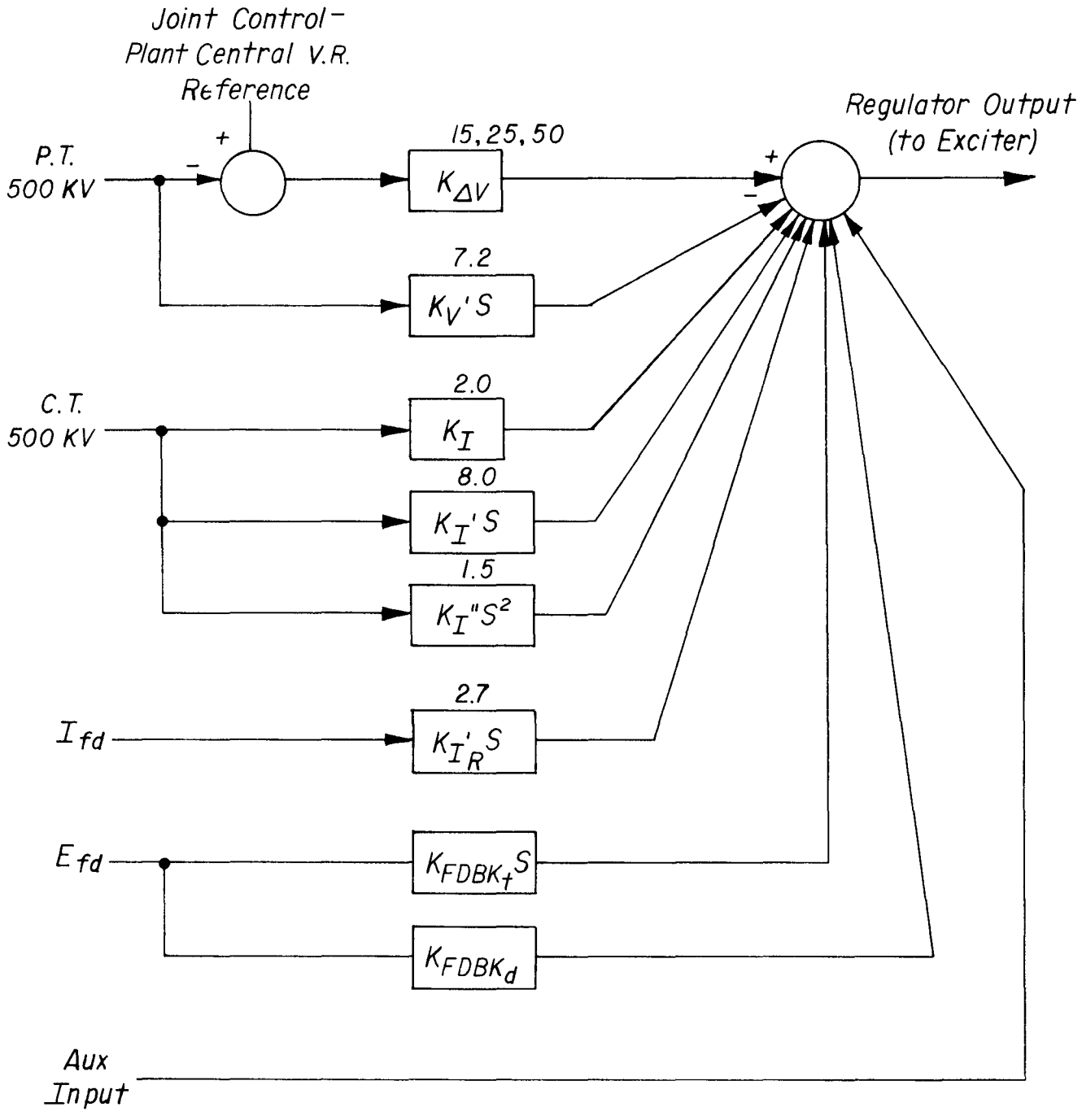

Figure 21. – Block diagram of existing regulator.

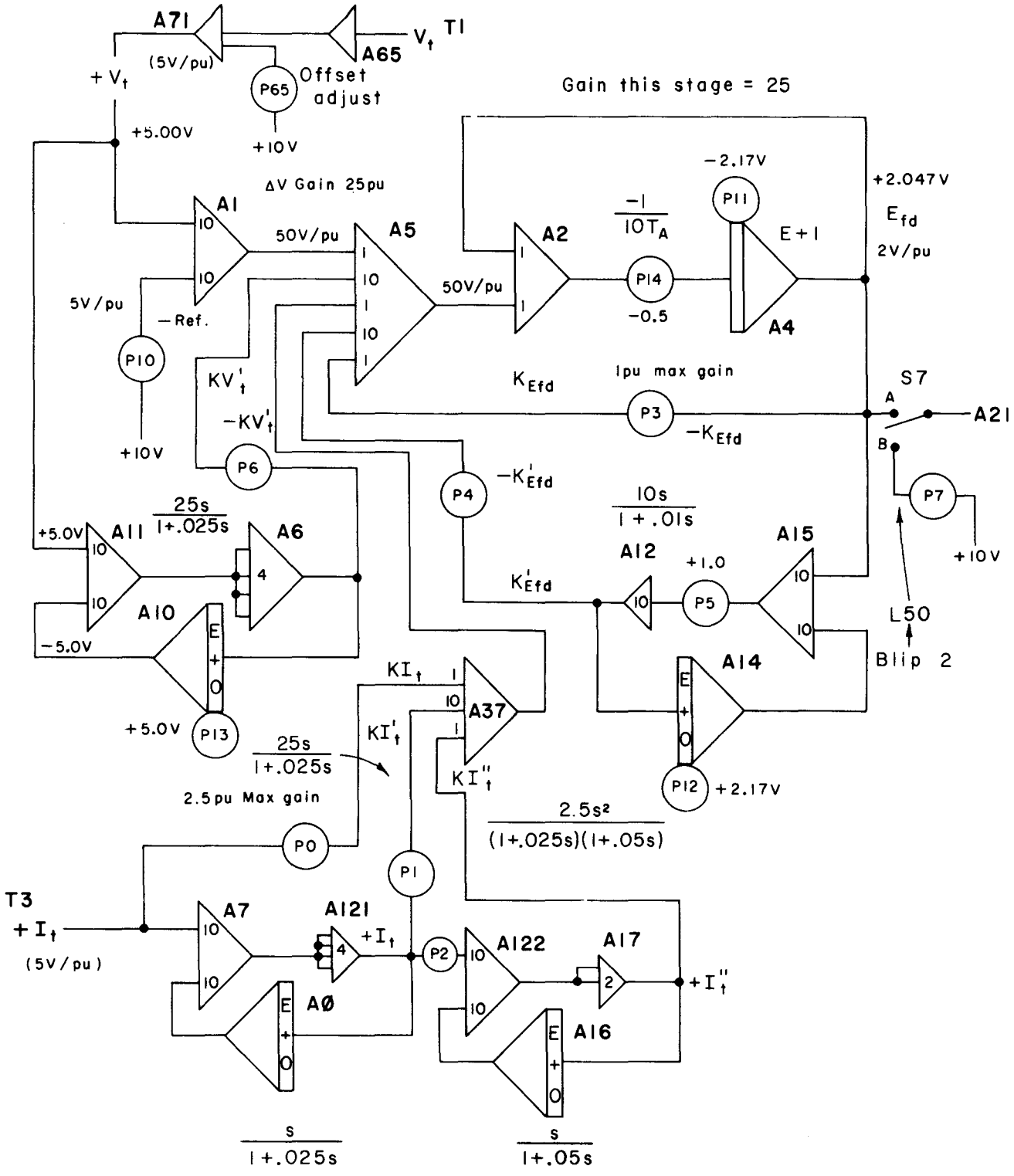

Figure 22. – Analog computer diagram of existing regulator.

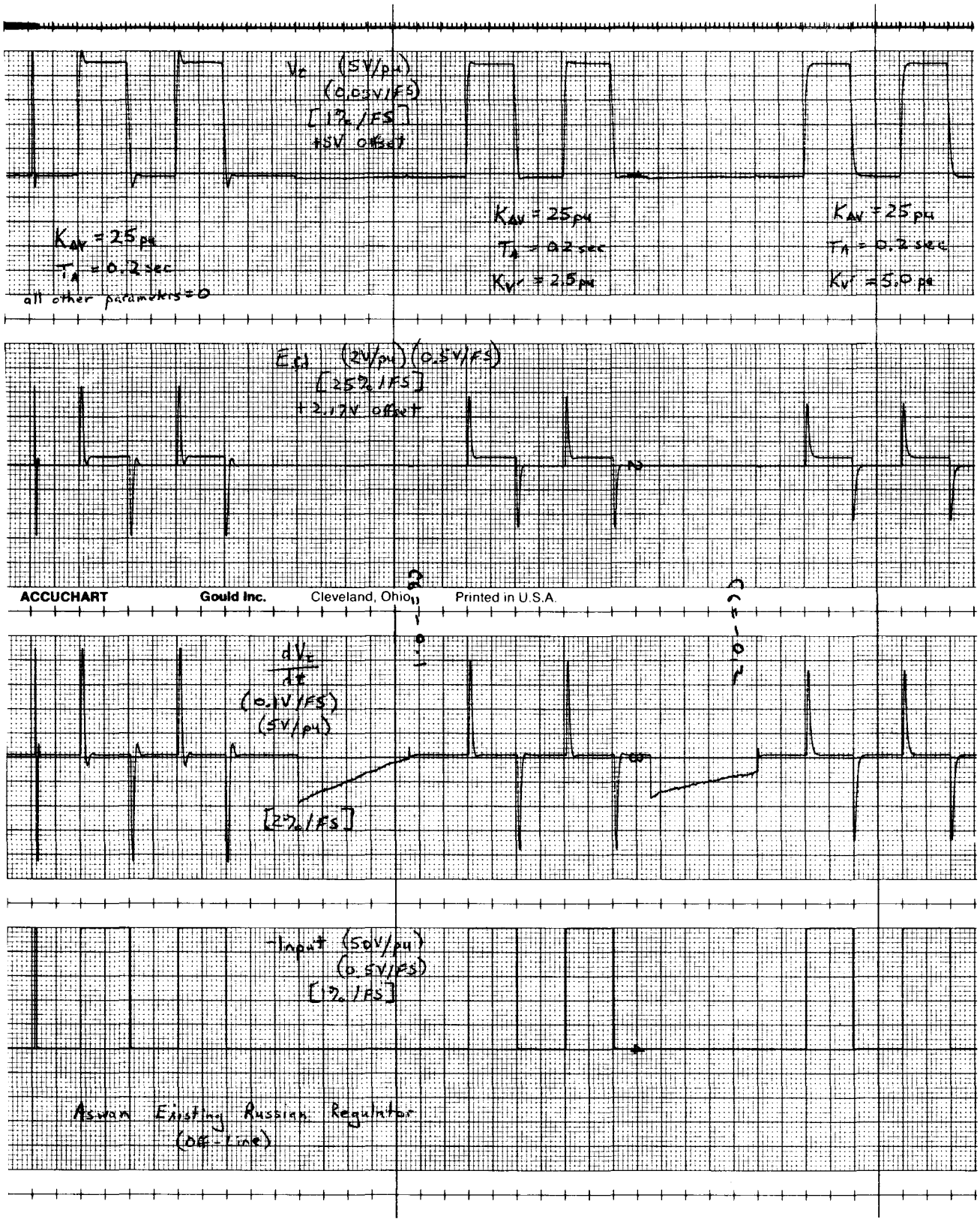

Figure 23. – Off-line time-domain responses of the existing regulator (sheet 1 of 2).

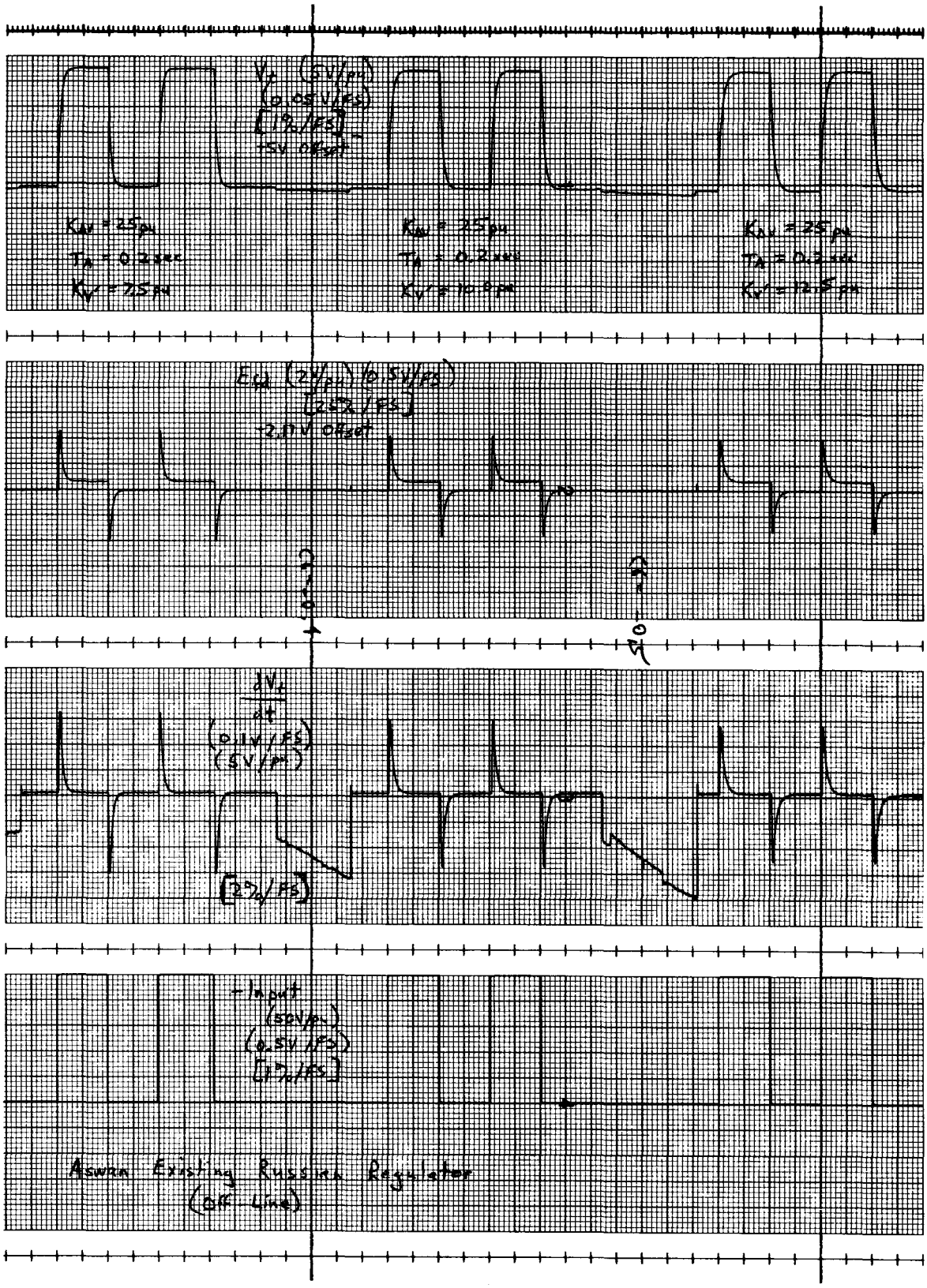

Figure 23. – Off-line time-domain responses of the existing regulator (sheet 2 of 2).

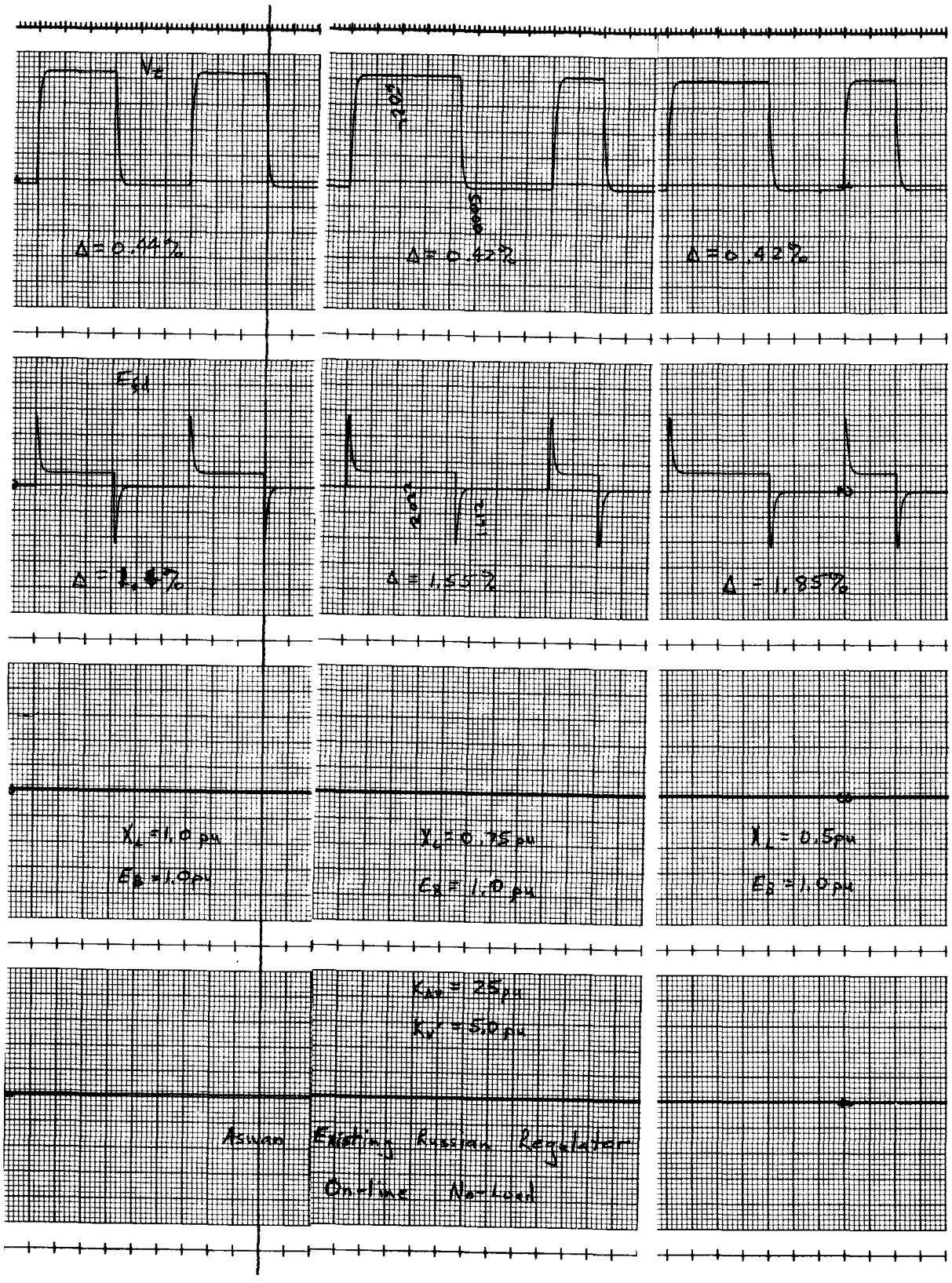

Figure 24. – On-line time-domain responses of the existing regulator (sheet 1 of 2).

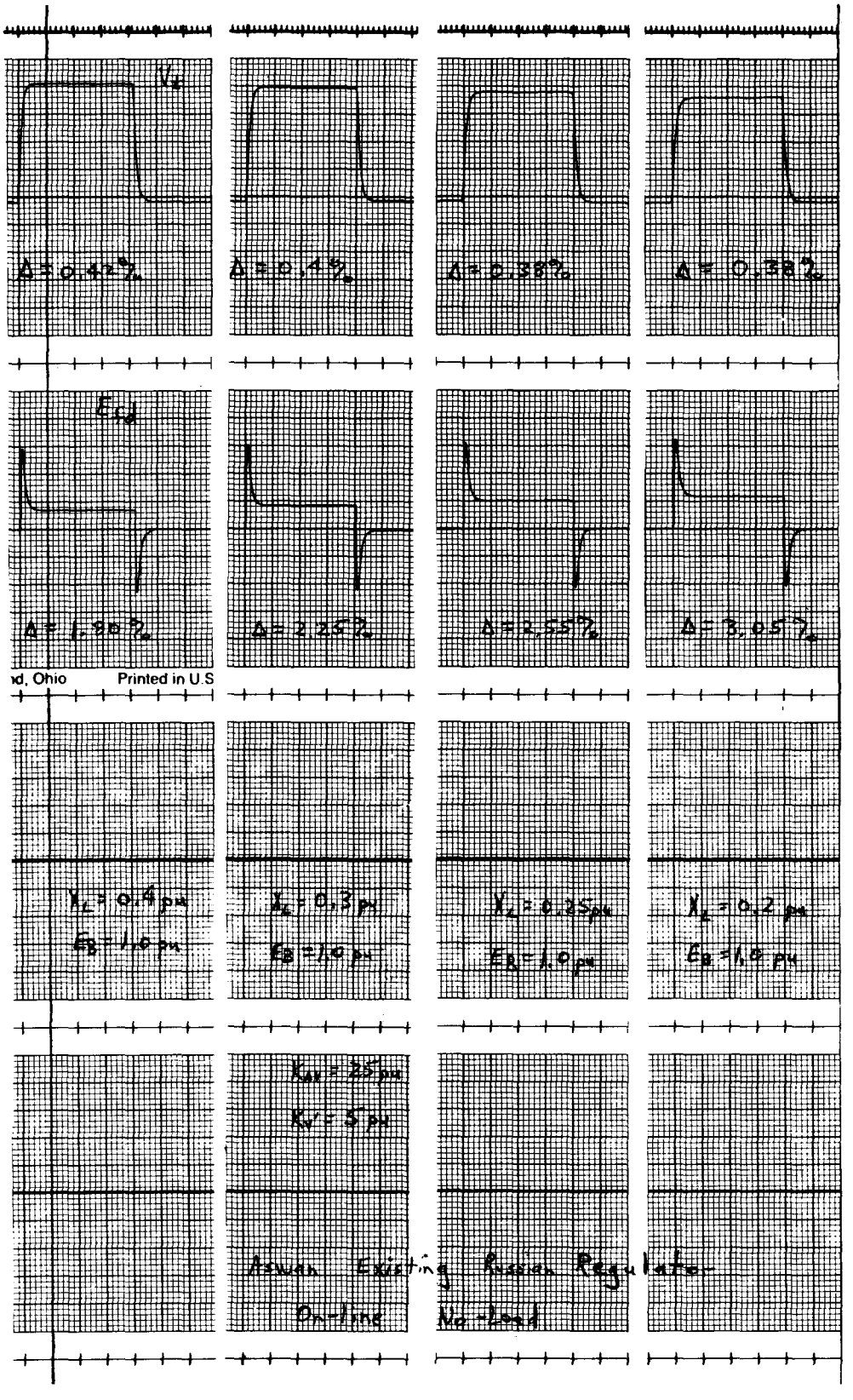

Figure 24. – On-line time-domain responses of the existing regulator (sheet 2 of 2).

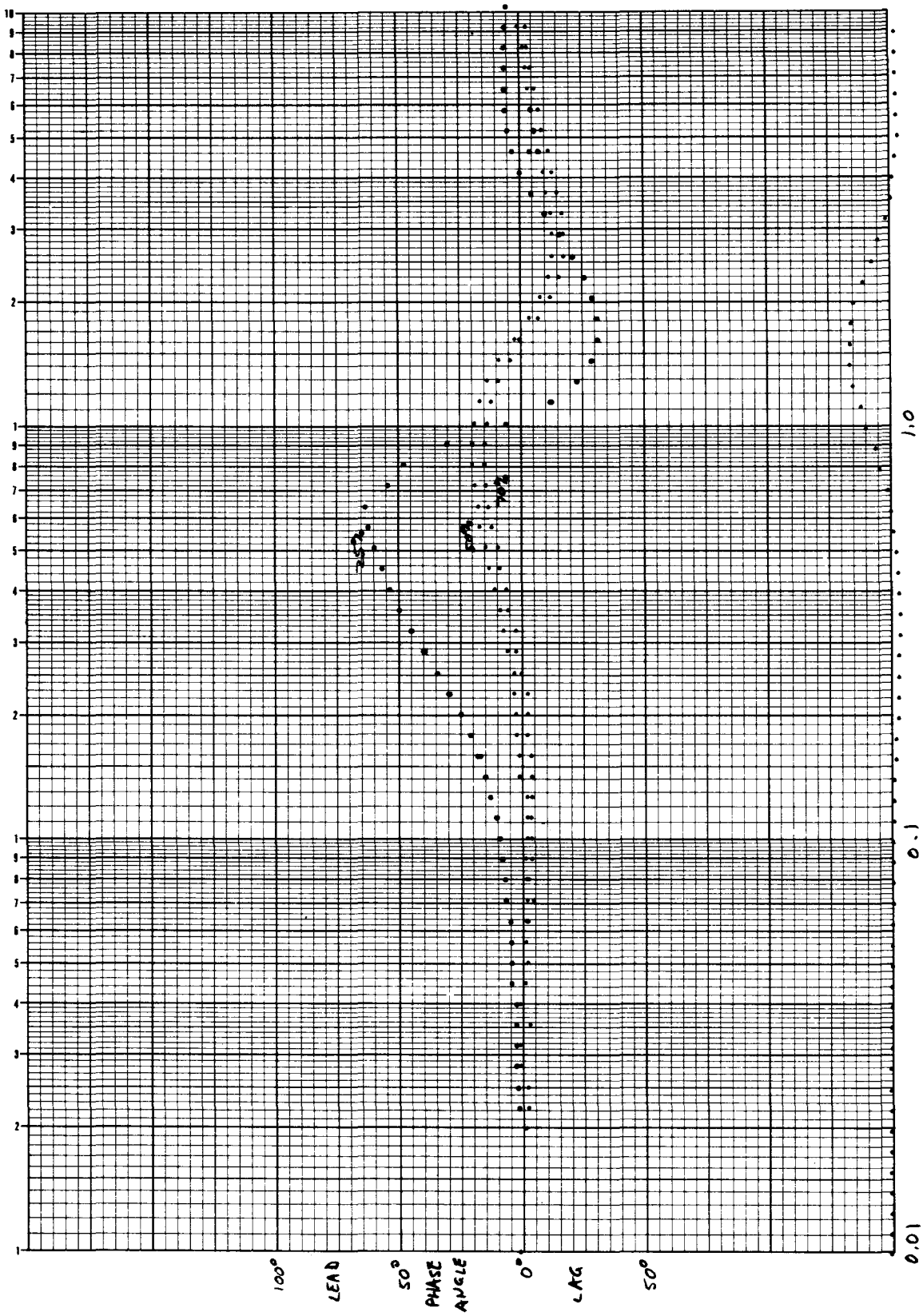

Figure 25. – Phase angle response of machine power to rotor position for various line impedances to the infinite bus.

APPENDIX A

NETWORK REDUCTION OF THE 500-kV SYSTEM

Appendix A

Network Reduction of the 500-kV System

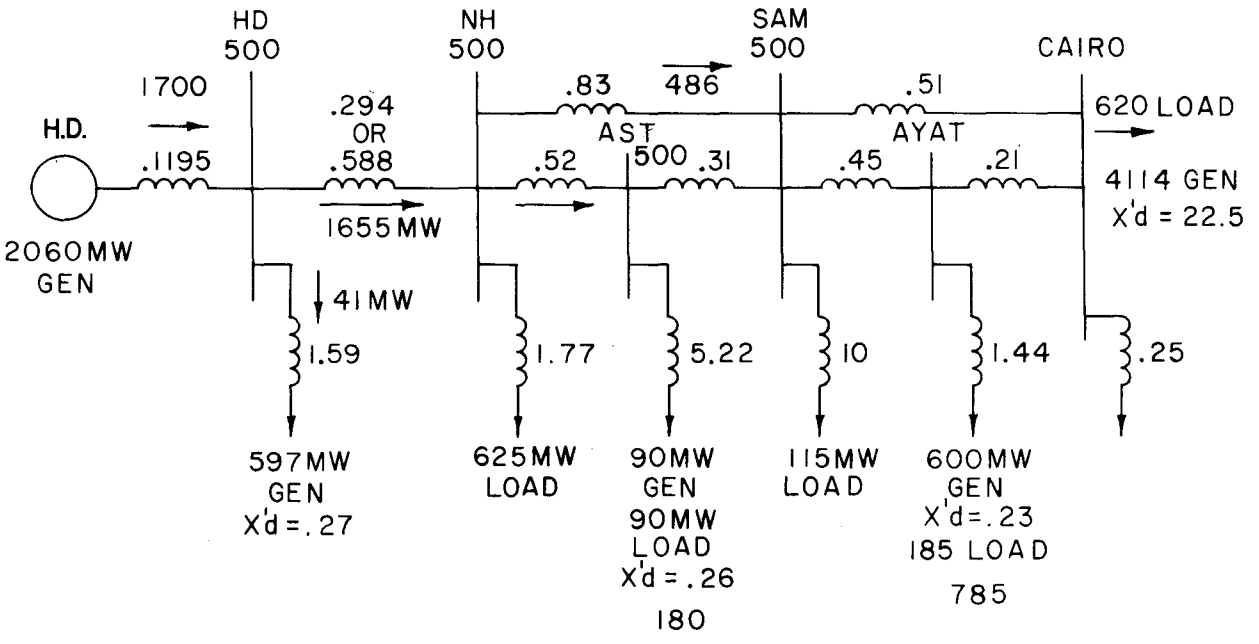

Unit Xfmr .097 on 600 MVA
500/130 Xfmr .095 on 600 MVA
X'd .27 on 600 MVA
Neglect lines
total .462 on 600 MVA
1.59 on 2060 MVA

(a) Step 1

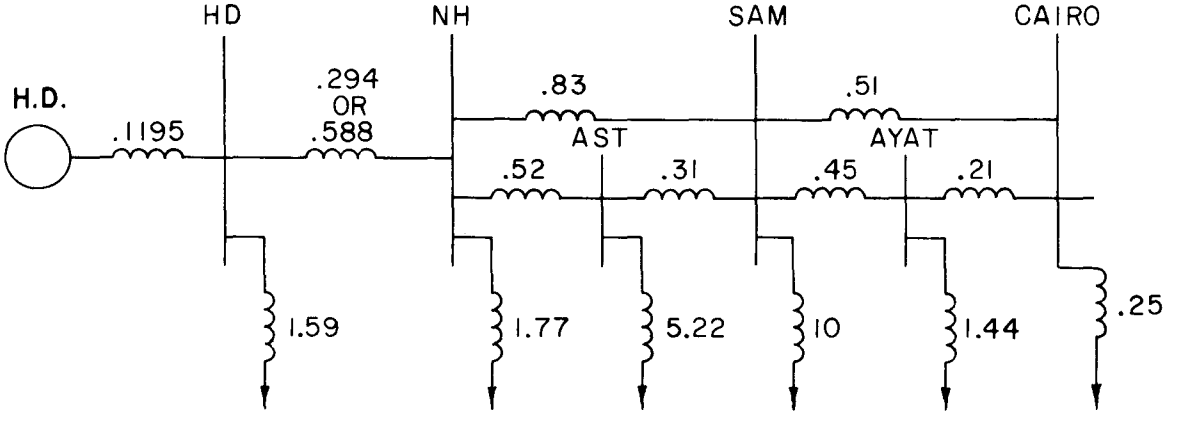

(b) Step 2

Figure A1. – Successive steps in reduction of equivalent circuits.

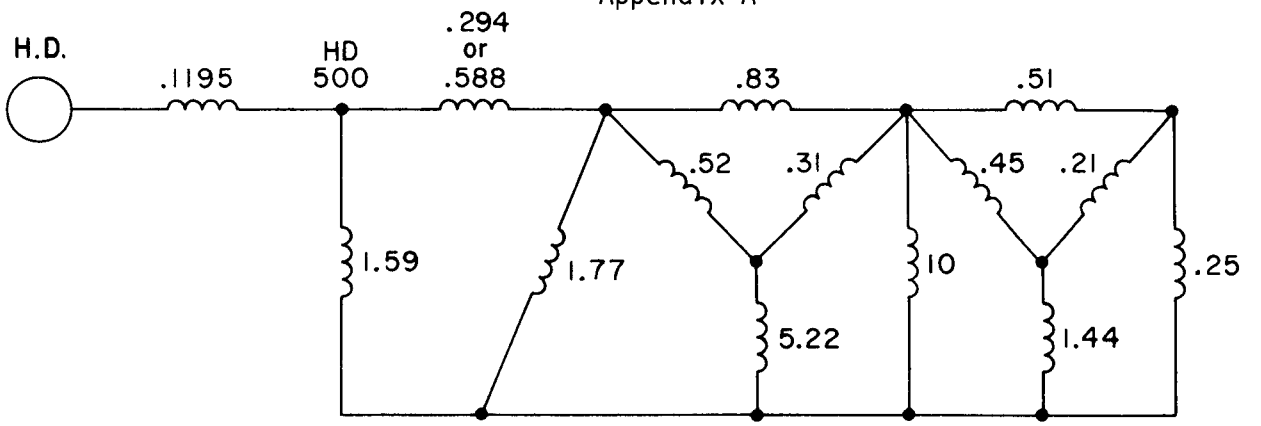

(c) Step 3

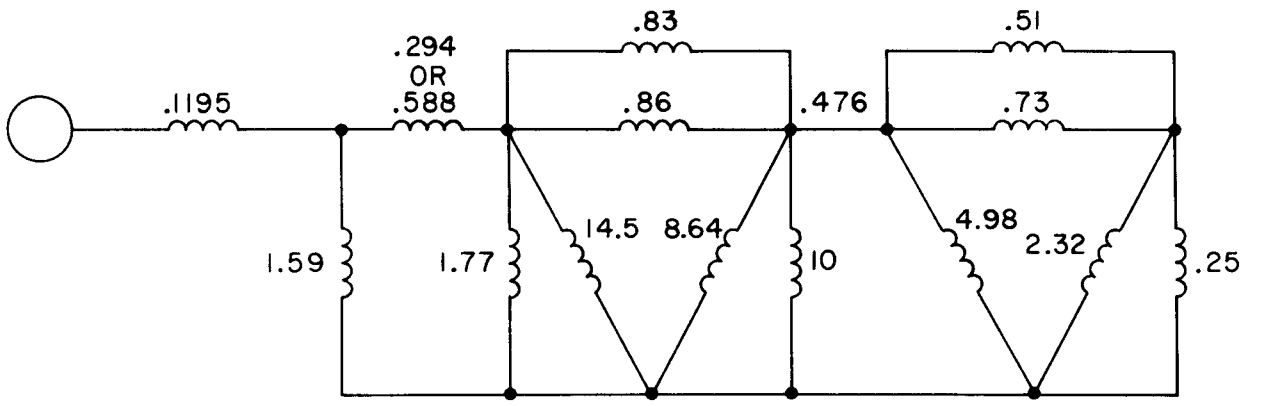

(d) Step 4

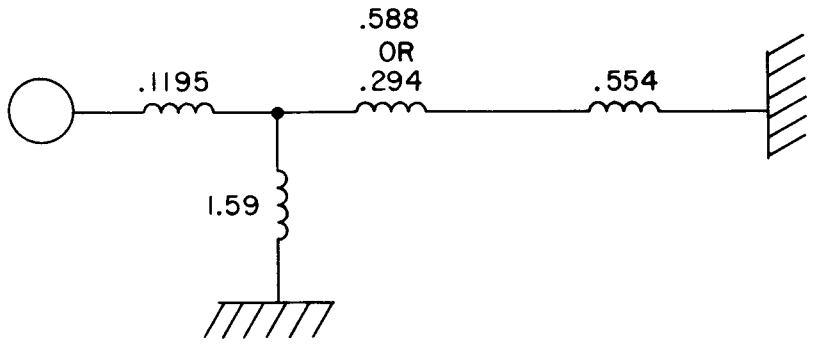

(2637 MW)

Weak System ⟶ 0.784 $P_{max} = 1.28_{py}$

Strong System 0.673 $P_{max} = 1.49_{py}$

(3061 MW)

(e) Step 5

Figure A1. – Successive steps in reduction of equivalent circuits – Continued.

APPENDIX B

ADDITIONAL ANALOG DIAGRAMS

Appendix B

Additional Analog Diagrams

$$P = E_{Bd} I_{Bd} + V_{Bq} I_{Bq}$$

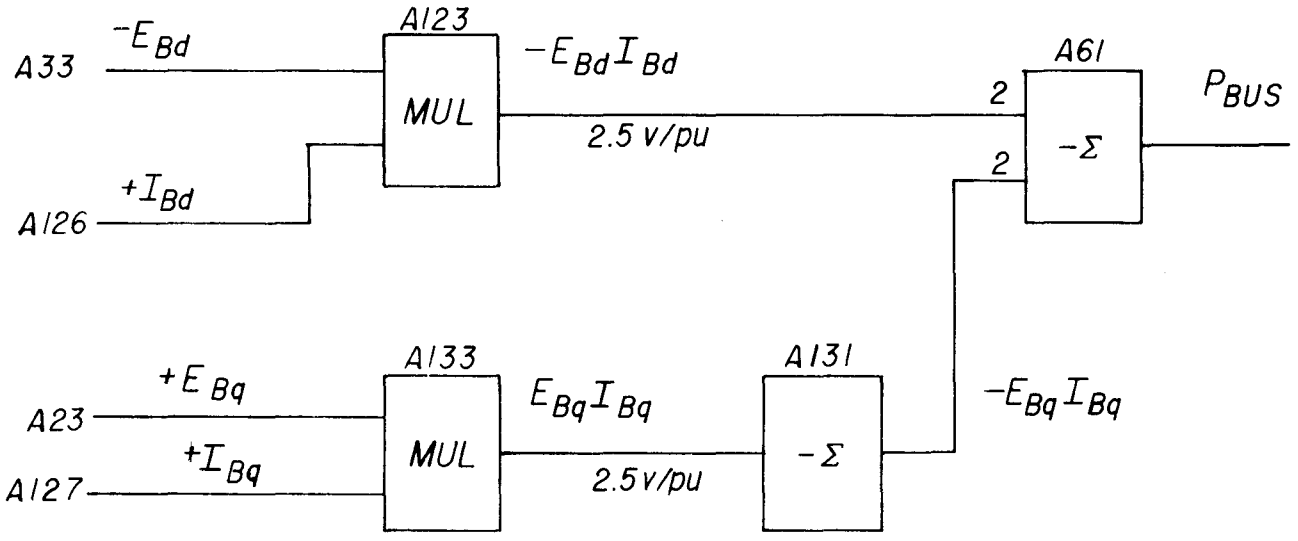

Figure B1. – Analog computer diagram of power to the infinite bus.

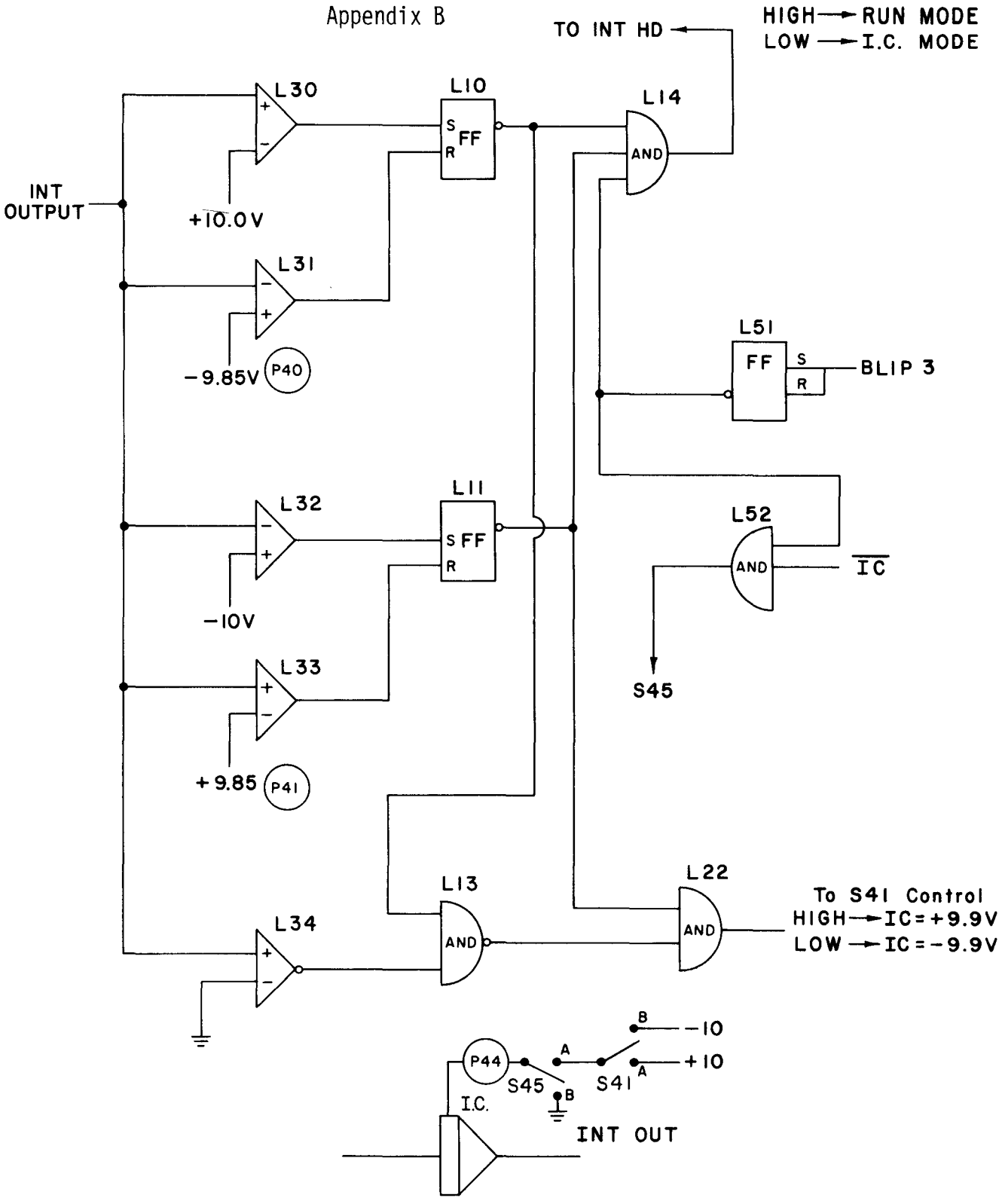

Figure B2. – Analog computer diagram to enable pole-slipping.

APPENDIX C

LISTING OF ANALOG COMPUTER CONSTANTS

Appendix C

Listing of Analog Computer Constants

```
1QT
1CL
1E0
1C000 = +0.1019
1C001 = +0.2019
1C002 = +0.0018
1C003 = -0.0000
1C004 = -0.0001
1C005 = +0.9994
1C006 = -0.4006
1C007 = +0.2171
1C010 = -0.5228
1C011 = -0.2166
1C012 = +0.0000
1C013 = +0.4999
1C014 = -0.5001
1C015 = +0.3301
1C016 = +0.0094
1C017 = -0.0009
1C020 = -0.5000
1C021 = +0.2936
1C022 = -0.2954
1C023 = +0.1948
1C024 = +0.4998
1C025 = -0.1666
1C026 = -0.6394
1C027 = +0.3279
1C030 = +0.3604
1C031 = +0.2390
1C032 = +0.0000
1C033 = -0.1000
1C034 = -0.4212
1C035 = +0.2400
1C036 = -0.1285
1C037 = +0.2000
1C040 = -0.9850
1C041 = +0.9850
1C044 = +0.9900
1C045 = +0.0000
1C050 = -0.0100
1C051 = +0.0000
1C054 = +0.0000
1C055 = +0.0000
1C060 = +0.5000
1C061 = -0.6888
1C064 = +0.0000
1C065 = +0.0030
1C070 = -0.0000
1C071 = +0.0000
1C074 = +0.5000
1C075 = +0.5000
1C100 = +0.3100
1C101 = -0.0769
1C102 = -0.0769
1C103 = +0.2540
1C104 = -0.1251
1C105 = -0.1251
1C106 = +0.9999
1C107 = +0.0000
1C110 = -0.5175
1C111 = -0.2168
1C112 = +0.2169
1C113 = +0.2170
1C114 = -0.2000
1C115 = +0.0000
1C116 = +0.0000
1C117 = +0.0000
1C120 = +0.0000
1C121 = +0.0000
1C122 = +0.0000
1C123 = +0.0000
1C124 = +0.0000
1C125 = +0.0000
1C126 = +0.0000
1C127 = +0.0000
1C130 = +0.0000
1C131 = +0.0000
1C132 = -0.7074
1C133 = -0.7075
1C134 = -0.6700
1C135 = -0.6700
1C136 = -0.0000
1C137 = +0.0000
1RV00=00000
1RV01=00000
1RV02=00000
1RV04=00000
1RV05=00000
1RV06=32624
1RV10=00000
1RV11=30672
1RV12=32760
1RT0=00500
1RT1=05000
1RT2=00000
1I000=E+0
1I004=E+1
1I010=E+0
1I014=E+0
1I016=E+0
1I020=E+0
1I024=E+2
1I030=E+2
1I034=E+1
1I036=E+2
1I040=E+0
1I044=E+0
1I050=E+0
1I054=E+0
1I060=E+0
1I064=E+0
1I070=E+0
1I074=E+0
1I100=E+0
1I104=E+2
1I110=E+0
1I114=E+0
1I120=E+2
1I124=E+2
1I130=E+0
1I134=E+0
1F00:
1B=41
1V01=-0.8682
1V02=-0.8212
1V03=-0.7756
1V04=-0.7315
1V05=-0.6890
1V06=-0.6481
1V07=-0.6086
1V08=-0.5707
1V09=-0.5343
1V10=-0.4995
1V11=-0.4661
1V12=-0.4344
1V13=-0.4041
1V14=-0.3754
1V15=-0.3482
1V16=-0.3225
1V17=-0.2984
1V18=-0.2758
1V19=-0.2547
1V20=-0.2352
1V21=-0.2171
1V22=-0.2007
1V23=-0.1857
1V24=-0.1723
1V25=-0.1604
1V26=-0.1500
1V27=-0.1400
1V28=-0.1300
1V29=-0.1200
1V30=-0.1100
1V31=-0.1000
1V32=-0.0900
1V33=-0.0800
1V34=-0.0700
1V35=-0.0600
1V36=-0.0500
1V37=-0.0400
1V38=-0.0300
1V39=-0.0200
1V40=-0.0100
1V41=+0.0000
1S;
1XT
```

```
+++++++++++++++++++++++++++++++++++++++++++++++++
+++++++++++++++++++++++++++++++++++++++++++++++++
+                                               +
+                ASWAN HIGH DAM                 +
+                                               +
+    GEN  INF BUS  TIELINE  MIDPT LOAD           +
+                                               +
+                MAY/JUNE  1984                 +
+                                               +
+                    JCA                        +
+                                               +
+++++++++++++++++++++++++++++++++++++++++++++++++
+++++++++++++++++++++++++++++++++++++++++++++++++
```

Figure C1. – Analog computer constants.

GPO 849-172

Mission of the Bureau of Reclamation

The Bureau of Reclamation of the U.S. Department of the Interior is responsible for the development and conservation of the Nation's water resources in the Western United States.

The Bureau's original purpose "to provide for the reclamation of arid and semiarid lands in the West" today covers a wide range of interrelated functions. These include providing municipal and industrial water supplies; hydroelectric power generation; irrigation water for agriculture; water quality improvement; flood control; river navigation; river regulation and control; fish and wildlife enhancement; outdoor recreation; and research on water-related design, construction, materials, atmospheric management, and wind and solar power.

Bureau programs most frequently are the result of close cooperation with the U.S. Congress, other Federal agencies, States, local governments, academic institutions, water-user organizations, and other concerned groups.

A free pamphlet is available from the Bureau entitled "Publications for Sale." It describes some of the technical publications currently available, their cost, and how to order them. The pamphlet can be obtained upon request from the Bureau of Reclamation, Attn D-822A, P O Box 25007, Denver Federal Center, Denver CO 80225-0007.